Gene-environment interactions in antisocial behavior are mediated by early-life 5-HT$_{2A}$ receptor activation

Sean C Godar[1,2], **Laura J Mosher**[1,3], **Simona Scheggi**[1,4], **Paola Devoto**[5], **Kelly M Moench**[6], **Hunter J Strathman**[1,3], **Cori M Jones**[3], **Roberto Frau**[5], **Miriam Melis**[5], **Carla Gambarana**[4], **Brent Wilkinson**[7], **M Graziella DeMontis**[4], **Stephen C Fowler**[3], **Marcelo P Coba**[7], **Cara L Wellman**[6], **Jean C Shih**[8], **Marco Bortolato**[1,2,*]

[1]Dept. of Pharmacology and Toxicology, University of Utah, Salt Lake City (UT), USA

[2]Consortium for Translational Research on Aggression and Drug Abuse (ConTRADA), University of Kansas, Lawrence (KS), USA

[3]Dept. of Pharmacology and Toxicology, University of Kansas, Lawrence (KS), USA

[4]Dept. of Molecular and Developmental Medicine, University of Siena, Italy

[5]Dept. of Biomedical Sciences, Section of Neuroscience, UNICA, Monserrato, Italy

[6]Dept. of Psychological and Brain Sciences, Program in Neural Science and Center for the Integrative Study of Animal Behavior, Indiana University, Bloomington (IN), USA

[7]Zilkha Neurogenetic Institute and Dept. of Psychiatry and Behavioral Sciences, University of Southern California, Los Angeles (CA), USA

[8]Depts. of Pharmacology and Pharmaceutical Sciences and Integrated Anatomic Sciences, University of Southern California, Los Angeles (CA), USA

Abstract

The ontogeny of antisocial behavior (ASB) is rooted in complex gene-environment (G×E) interactions. The best-characterized of these interplays occurs between: a) low-activity alleles of the gene encoding monoamine oxidase A (*MAOA*), the main serotonin-degrading enzyme; and b) child maltreatment. The purpose of this study was to develop the first animal model of this G×E interaction, to help understand the neurobiological mechanisms of ASB and identify novel targets for its therapy. *Maoa* hypomorphic transgenic mice were exposed to an early-life stress regimen consisting of maternal separation and daily intraperitoneal saline injections and were then compared with their wild-type and non-stressed controls for ASB-related neurobehavioral phenotypes. *Maoa* hypomorphic mice subjected to stress from postnatal day (PND) 1 through 7 –

Correspondence to: Marco Bortolato, MD PhD, Dept of Pharmacology and Toxicology, College of Pharmacy, University of Utah, Skaggs Hall, Room 3916, 30 S 2000 E, Salt Lake City (UT) 84112, Phone: 801-587-3352 Fax: 801-585-5111 marco.bortolato@utah.edu.

but not during the second postnatal week - developed overt aggression, social deficits and abnormal stress responses from the fourth week onwards. On PND 8, these mice exhibited low resting heart rate - a well-established premorbid sign of ASB – and a significant and selective up-regulation of serotonin 5-HT_{2A} receptors in the prefrontal cortex. Notably, both aggression and neonatal bradycardia were rescued by the 5-HT_2 receptor antagonist ketanserin (1–3 mg kg^{-1}, IP), as well as the selective 5-HT_{2A} receptor blocker MDL-100,907 (volinanserin, 0.1–0.3 mg kg^{-1}, IP) throughout the first postnatal week. These findings provide the first evidence of a molecular basis of G×E interactions in ASB and point to early-life 5-HT_{2A} receptor activation as a key mechanism for the ontogeny of this condition.

Keywords

Antisocial behavior; gene-environment interactions; aggression; serotonin; animal models

1. Introduction

Antisocial behavior (ASB) is characterized by a complex pattern of overt and covert hostility, often resulting in aggression toward others, property damage, and rule violations. As such, it imposes a substantial burden on society and public health (Whitehead *et al.*, 2003; Shepherd *et al.*, 2004), on account of the robust association of ASB with delinquency and violent crimes (Shader *et al.*, 2003; Stone, 2007), as well as a broad spectrum of psychiatric disorders (Sher *et al.*, 2015). Although no medications are currently approved for ASB, several drugs, including lithium, anticonvulsants, sedatives, antipsychotics, and antidepressants, are used to reduce aggression (Fava, 1997; Khalifa *et al.*, 2010), but are often inadequate and associated to significant adverse events. This scenario underscores the urgent need for novel tools for ASB prevention and treatment; current efforts to develop such interventions, however, are undermined by our limited understanding of ASB neurobiology.

Animal models focusing on the impact of either genetic or environmental variables on fighting and hostile social behavior have proven crucial to investigate the neurobiology of aggression; from a translational perspective, however, these monofactorial approaches largely fail to capture the biosocial origin of ASB, which reflects complex gene-by-environment (*G×E*) interactions (Raine, 2002). The best-characterized among these interplays occurs between child maltreatment and the gene encoding monoamine oxidase A (*MAOA*) (Caspi *et al.*, 2002), the main serotonin (5-HT) catabolic enzyme (Bortolato *et al.*, 2008). The function of *MAOA* is influenced by a 30-bp variable tandem repeat (VNTR) sequence located upstream of its promoter; depending on the number of repeat sequences, alleles have either high (3.5 or 4 repeats, present in more than 60% of men) or low (2 or 3 repeats, present in more than 35%) transcriptional activity (Sabol *et al.*, 1998; Godar *et al.*, 2016). In 2002, Caspi and colleagues documented that low *MAOA* variants increased the risk of ASB in boys subjected to abuse and neglect (Caspi *et al.*, 2002). Although this *G×E* interaction has been substantially confirmed by most follow-up studies and meta-analyses (Kim-Cohen *et al.*, 2006; Fergusson *et al.*, 2011; Byrd and Manuck, 2014) - but see Haberstick et al (2014) for contrasting evidence -, the biological mechanisms whereby

MAOA variants shape the long-term behavioral consequences of child maltreatment remain completely unknown.

Here, we developed a novel model of this $G \times E$ interaction to better understand its molecular mechanisms underpinning. As no functional VNTR *Maoa* polymorphisms have been documented in mice, we mimicked *MAOA* low-activity carriers by using MAOA^{Neo}, a line of transgenic *Maoa* mouse mutants previously developed by our group, which exhibits low enzymatic activity but no spontaneous aggression (Bortolato *et al.,* 2011). These animals were subjected to early-life stress (ES) to reproduce the impact of child abuse and neglect; to validate the translational relevance of this model of $G \times E$ interactions, we examined the temporal trajectory of its aggressive responses, as well as the accompanying phenotypic signs. Next, we investigated the critical period for ES to result in aggressive behavior in our model. Finally, we studied the molecular mechanisms mediating this $G \times E$ interaction and assessed which premorbid signs may predict aggression in these models to gain insight into potential interventions that may prevent ASB before its clinical onset. Given that ES-subjected MAOA^{Neo} pups exhibited a significant upregulation of 5-HT$_{2A}$ receptors in the prefrontal cortex (PFC), we then evaluated the implications of these molecules in the pathogenesis of ASB-related behaviors.

2. Materials and Methods

2.1 Animals

Male MAOA^{Neo} mice were generated from mating primiparous MAOA^{Neo} heterozygous (HZ) females with wild-type (WT) sires, as previously described (Bortolato *et al.,* 2011). Since *Maoa* is an X-linked gene, male offspring of MAOA^{Neo} HZ dams were either MAOA^{Neo} or WT. Pregnant dams were singly-housed 3 days prior to parturition. Only litters with > 4 pups (and at least 2 males) were used, and all litters with more than 8 pups were culled to eight at postnatal day (PND) 1 to assure uniformity of litter size. Bedding was changed in all cages at PND 7 and PND 14, and mice were weaned at PND 21. Animals were housed in a room maintained at 22°C, on a 12 h: 12 h light/dark cycle from 8 am to 8 pm. Food and water were available *ab libitum*. All experimental procedures were executed in compliance with the National Institute of Health guidelines and the EU Directive 2010/63 and approved by the Animal Use Committees of each Institution. Throughout all studies, every effort was made to minimize the number and suffering of animals used.

2.2 Drugs

The prototypical 5-HT$_2$ receptor antagonist ketanserin (Leysen et al., 1981) (KET, 1–3 mg kg^{-1}, IP, 10 μl g^{-1} body weight; Sigma-Aldrich, St.Louis, MO, USA) and the highly selective 5-HT$_{2A}$ receptor blocker MDL-100,907 (volinanserin; MDL, 0.1–0.3 mg kg^{-1}, IP, 10 μl g^{-1} body weight; Sigma-Aldrich, St. Louis, MO, USA) were dissolved in 5% Tween-80 and brought to volume with saline solution. Given that both compounds are competitive antagonists, the effects of two separate doses were tested, to account for variations in 5-HT levels in MAOA^{Neo} mice. Doses were selected based on available evidence on the range of efficacy in mouse models.

2.3. Behavioral procedures and testing paradigms.

Behavioral experiments occurred between 11 am and 5 pm during the light phase of the light-dark cycle. All experiments were conducted on groups comprised of subjects from at least 5 litters, and randomly assigned to each group. Group size was determined based on power analyses based on preliminary results. To ensure scientific rigor, all analyses were performed by investigators blinded to genotypes and treatment groups.

2.3.1 Early Stress—To simulate child abuse and neglect, pups were initially subjected to a daily stress regimen of maternal separation (MS, for 2–4 h/day), saline intraperitoneal injections (SI, executed with body restraint via dorsal pinch) or the combination of both stressors, during different early-life developmental periods. Specifically, in the first experiment aimed at the validation of the model, all three regimens were administered from PND 1 through 21; subsequently, only the combination of MS and SI was administered on PND 1–7 or PND 8–14. The selection of SI as a stressor was based on previous literature validating the robust stressful effects of this procedure in mice (Ryabinin *et al.,* 1999). Manipulations were performed in a pseudorandom, unpredictable fashion, with pups subjected to different durations of MS and at different times. For each procedure, male pups were removed from their nest and placed into a new cage in a separate temperature-controlled (25°C) room, by both male and female personnel. SI were performed using a microinjector connected to a Hamilton syringe (10 μl g^{-1} body weight). The stressfulness of each intraperitoneal injection was always ensured by verifying the response from each pup (typically consisting of rapid limb and head movements after the puncture). Non-stressed control pups were briefly removed from their cages and returned to their home cage after brief handling. All pups in each litter were subjected to the same manipulation; to control for litter effects, each experimental group included mice from at least 5 litters. While ES was applied to both male and female pups within the same litter (to standardize conditions irrespective of sex distribution and avoid potential errors in sex identification during the first week of postnatal life), only males were used in the study, given the marked male preponderance of ASB (Compton *et al.,* 2005).

2.3.2 Maternal behaviors—To rule out abnormalities in maternal care of MAOA^{Neo} HZ mothers, maternal behaviors were measured daily, as previously indicated (Romeo *et al.,* 2003) under red-light settings from PND 1 through 7. Behaviors were assessed once per min for 30 min before and immediately after maternal separation (or brief handling for non-stressed control litters). Behaviors were categorized as: 1) off-nest; 2) arched-back (active) nursing; 3) prone (passive/inactive) nursing; 4) pup licking and grooming; 5) nest-building; 6) other behaviors (including non-maternal behaviors on nest, such as self-grooming).

2.3.3 Developmental milestones—Assessment of early postnatal developmental milestones focused on the evaluation of righting reflex and negative geotaxis throughout the first week (Heyser, 2003). Righting reflex was tested by gently placing each pup on its back and measuring its latency to regain its natural position with all paws on the platform. Negative geotaxis was tested by orienting each pup downward on an inclined plane (with a 30° slope); the latency of the mouse to reorient itself in an upward facing position was

recorded. Both reflexes were tested on a platform kept at 32°C to prevent hypothermia. A 60-s cut-off time was used.

2.3.4   Electrocardiogram (ECG)—Heart rate and dynamics were measured in male pups on PND 8, via a non-invasive, two-lead system recording from the paws (ECGenie, Mouse Specifics, Framingham, MA, USA) as previously detailed (Chu *et al.,* 2001). The apparatus consisted of a platform embedded with ECG electrodes that was kept in an isolation cabinet maintained at a temperature of 32°C. To minimize separation-induced stress, pups were individually placed on the platform with a small amount of home cage bedding. Pup ECGs were recorded for 5 minutes. Since movement could interfere with the fidelity of the ECG data, recording sequences that exhibited little noise and lasted between 2–10 s were selected for subsequent analyses. At least 5 sequences were selected for each animal across the entire session. ECG sequences were individually analyzed by eMouse software (Mouse Specifics, Framingham, MA, USA) and averaged for each animal. Physiological measures included heart rate (based on the evaluation of R-R interbeat intervals) as well as QRS intervals.

2.3.5   Locomotor activity—Locomotor activity in male pups (PND 8) was assessed through a custom square force-plate actometer (Fowler *et al.,* 2001), specifically designed for monitoring pup movements. The actometer measured 12×12 cm and was surrounded by 20 cm-high clear Plexiglas walls. The four force transducers (Model 31A, Honeywell/ Sensotec) that supported the load plate at its corners were sampled 100 times/s, giving a temporal resolution of 0.01 s. Force resolution was 0.1-g force, and spatial resolution was about 2 mm. The mass of the load plate was 20.1 g. A Pascal program written in-house directed the timing and data-logging processes via a LabMaster interface connected to a computer. The actometer surface was warmed with a heating lamp to 32°C to prevent hypolocomotion due to poor thermoregulation in mouse pups.

On PND 28 and 80, locomotor activity was examined in an open field, as previously reported (Bortolato *et al.,* 2011). The open field apparatus was a square, beige arena (measuring 20×20 and 40×40 for 28- and 80-day old mice, respectively) surrounded by four black Plexiglas walls (30 and 40 cm high, respectively). Animals were individually placed onto the center of the floor and allowed to explore for 5 min. The total distance, time spent in the center and percent locomotor activity in the center were recorded and calculated by Ethovision behavioral tracking software (Noldus, Wageningen, The Netherlands).

2.3.6.   Ultrasonic vocalizations—Ultrasonic vocalizations were assessed in pups on PND 8 as previously described (Bortolato *et al.,* 2013a). Pups were individually placed in a cylindrical cell composed of stainless steel rods (8 cm in diameter $\times$ 8 cm in height), located in a sound-attenuating cabinet. A heating lamp (set to 32°C) was located overhead to limit potential confounds due to alterations in body temperature. Ultrasonic vocalizations were recorded for 5 min using a high-quality condenser microphone (Avisoft Bioacoustics, Berlin, Germany) suspended 5 cm above the cell. Spectrograms were generated by Fourier transformation using Avisoft-SAS Lab Pro software. High and low frequency thresholds were set at 100 and 15 kHz respectively. Calls were detected through an automated algorithm using an amplitude threshold of 35–45 db (depending on background noise)

relative to maximum spectrogram intensity and a hold time of 40 ms. These parameters were optimized after a series of trials, and efficacy of call detection was verified manually by a trained observer. The total number of calls were recorded.

2.3.7. Novel object exploration—Novel-object exploration was tested as previously described (Godar *et al.,* 2011). Animals were tested for novelty-induced responses in the novel object exploration task in a dimly lit room (10 lux). Mice were briefly removed from their home cage, and two equivalent objects were placed in the cage at equal distances apart and from the sides. Mice were returned to the middle of their home cage and allowed to freely explore for 15 min. Different objects were used for animals at PND 28 and PND 80. Behavioral measures include the number and duration of object exploration (as defined by sniffing aimed at the object). Climbing behavior was not counted as exploration.

2.3.8. Light-dark box—Anxiety-related behaviors were measured using the light-dark box as previously described (Bortolato *et al.,* 2013b). Briefly, the apparatus consisted of two chambers of identical size ($20 \times 20 \times 30$ cm) separated by a doorway (8×10 cm): an uncovered white Plexiglas chamber, kept under a 200-lux light (light box); and a covered black Plexiglas dark chamber (dark box). Mice were individually placed against the far wall of the light chamber and allowed to explore the apparatus unimpeded for 10 min. Behavioral measures included the time spent in each chamber and the number of transitions between chambers.

2.3.9. Startle reflex and prepulse inhibition (PPI)—Startle reflex was measured as previously described (Bortolato *et al.,* 2013b), using 8 sound-attenuated chambers with fan ventilation (SR-LAB; San Diego Instruments, San Diego, CA, USA). Each chamber contained a Plexiglas cylindrical cage (diameter: 5 cm), mounted on a piezoelectric accelerometric platform connected to an analog-digital converter to record force responses. The response to each stimulus was recorded for 65 consecutive 1-ms readings. To ensure comparable sensitivities across chambers, we used a dynamic calibration system before each session. At the start of each session, animals received a 5-min acclimation consisting in 70-dB background white noise. Background white noise continued throughout the session. Following acclimation, animals were subjected to three consecutive blocks of pulse, prepulse + pulse and 'no stimulus' trials. During the first and the third block, animals received only five pulse-alone trials of 115 dB. Conversely, in the second block animals were exposed to a pseudorandom sequence of 50 trials, consisting of 12 pulse-alone trials, 30 trials of pulse preceded by 73, 76 or 82 dB pre-pulses intensities (10 for each level of prepulse loudness) and eight no stimulus trials, where only the background noise was delivered. Intertrial intervals were randomly selected between 10 and 15 s. Sound levels were assessed using an A-scale setting. Percent PPI was calculated with the following formula: %PPI= 100-(mean startle amplitude for prepulse-pulse trials / mean startle amplitude for pulse-alone trials) $\times$ 100. The five pulse-alone trials in the first and third blocks were excluded from the calculation. Percent PPI values were collapsed across prepulse intensity to represent average %PPI.

2.3.10 Tail suspension—The tail suspension test was performed as described elsewhere (Bortolato *et al.,* 2013b). Mice were individually suspended by the tail using medical tape affixed to a hook, at 30 cm from the floor. Environmental light was kept at 300 lux. Animals were videorecorded for 6 min, and the duration of immobility (s) was measured.

2.3.11. Spontaneous alternations in the T-maze—Spontaneous alternations in the T-maze were measured to test for perseverative behavior and working memory efficiency. Testing was performed in a black Plexiglas T-maze, as previously described (Bortolato *et al.,* 2013a). Each animal underwent 8 consecutive trials. At the start of each trial, the test animal was individually placed into the central 'start' arm for a 15-s acclimation. The black guillotine door was removed, and the animal was permitted to freely explore the two arms. Once the animal entered (with all four paws) one of the two alternative arms (left or right), the guillotine door of that arm was closed for 15 s to confine the animal. The animal was briefly removed from the apparatus and the T-maze was quickly cleaned and dried to remove any olfactory cue that may condition the performance in the next trial. A trial was considered failed if the animal did not enter an arm within 120 s. Mice that recorded two failures (1 *CTL*, 2 *E*, 3 *G* and 3 *G×E* animals) were removed from the study. The percentage of arm alternations was analyzed for each animal.

2.3.12. Resident-intruder aggression—Resident-intruder aggression was assessed as previously described (Bortolato *et al.,* 2011). Briefly, male mice were isolated in their home cages for 7 days to establish territorial behavior. An unfamiliar age- and weight-matched male conspecific was placed in the home cage and animals allowed to freely interact for 10 min. Behavioral measures included the latency to the first attack, the total number of attacks, and the overall duration of attack episodes. An attack was defined as a burst of bites, sideways threats, and rough grooming, initiated by the resident. Intruders were only used once to avoid potential stress carryover effects.

2.3.13. Social interaction—Social interaction was tested as previously described (Godar *et al.,* 2011). Briefly, a male test mouse and a novel age- and weight-matched male conspecific were simultaneously placed at the opposing ends of an unfamiliar cage and allowed to freely interact for 10 min. The frequency and overall duration of social interaction (defined as sniffing of the partner) approaches initiated by the test mouse were scored. Additionally, the different behavioral responses of the test mouse upon approaches initiated by the conspecific were assessed, including reciprocal social interaction; and non-reciprocal responses, consisting of: escaping/withdrawing reactions (during which the test mouse retreated in response to a social approach); freezing (total immobility except for breathing movements); offensive (tail rattling and chasing); and attacking (as defined above). To control for interindividual differences in the conspecific's sociability, each response was calculated as the ratio of these responses and the total number of approaches initiated by the partner (except for those instances during which the test mouse was engaged in other active, non-social behaviors, such as digging, grooming or rearing). Based on these measurements, an asociality index was also calculated with the following formula: Non-reciprocal responses / (Reciprocal + Non-reciprocal responses).

2.3.14.   Predator-cued emergence test—Threat assessment was studied by measuring the behavioral reactivity to an anesthetized rat, as previously described (Godar *et al.,* 2011). The apparatus consisted of a black Plexiglas L-shaped maze, kept in a room with very dim illumination (2 lux). One of the two arms contained a rectangular enclosure (10 × 10 × 20 cm), which was separated from the adjacent area by a guillotine door. An anesthetized rat was placed in the other arm, with the snout partially obstructing the intersection between arms, at 3 cm from the wall (Fig. 3a). A mouse was kept in the enclosure for 10 min, with the door kept closed. The door was then raised (~6 cm from the floor) and the mouse was permitted free access to explore all areas. Behavioral measures included latency to emerge from the start chamber, time spent in each chamber and the time spent actively exploring the rat (ie. sniffing, rearing and climbing).

2.4.   Neurochemical analyses

Neurochemical analyses were performed on mice on PND 8. Mice were sacrificed via decapitation and the PFC was rapidly removed, snap-frozen and stored at −80°C. For HPLC analyses in PND 8 pups, forebrain regions were extracted to obtain sufficient material for determination of monoamine content. Analyses were performed by investigators blinded to genotypes and treatment groups.

2.4.1   HPLC determination of monoamine content—Monoamine levels were measured using HPLC as previously indicated (Grappi et al., 2011). The PFC was homogenized in a solution containing 0.1 M trichloroacetic acid, 10 mM sodium acetate, and 0.1 mM EDTA; 1 μM isoproterenol was used as an internal standard. The homogenates were centrifuged, and the supernatants were collected for HPLC analyses. 5-HT, dopamine and norepinephrine (Sigma-Aldrich) were used as standards. 5-HT levels were quantitated using a mobile phase containing the homogenization buffer with 7% methanol. Dopamine and norepinephrine content were separately measured using a trichloroacetic acid mobile phase solution (without methanol). All mobile phases were filtered and de-aerated, and the pump speed (Shimadzu LC-6A liquid chromatograph, Columbia, MD, USA) was 1.5 ml/min. The reverse-phase column used was a Rexchrom S50100-ODS C18 column (Waters Corporation, Milford, MA, USA) with a length of 25 cm and an internal diameter of 4.6 mm. The compounds were measured at +0.7 V using a Shimadzu L-ECD-6A electrochemical detector.

2.4.2.   Western blotting—Western-blotting was performed as previously published (Scheggi et al., 2009). Briefly, for 5-HT receptors, samples were homogenized in ice-cold buffer containing 50 mM Tris-Cl, pH 7.4, 150 mM NaCl, 10% glycerol, 1% NP-40, 0.5% sodium deoxycholate, 0.1% SDS, and protease inhibitor cocktail as described (Yadav *et al.,* 2011). Equal amounts of protein (20 μg) were loaded onto each gel and proteins were separated and transferred onto nitrocellulose membranes according to standard protocols. Primary antibodies for 5-HT$_{1A}$ (Santa Cruz Biotechnologies, Santa Cruz, CA, USA), 5-HT$_{1B}$ (Santa Cruz Biotechnologies), 5-HT$_{2A}$ (Neuromics, Minneapolis, MN, USA) and 5-HT$_{2C}$ (Santa Cruz Biotechnologies) receptors were incubated in blocking buffer overnight at 4° C. Specific antibody binding was detected by chemiluminescence. Samples from each genotype, environment and treatment group were immunoblotted and analyzed together. To

control for equal loading, blots incubated with antibodies were stripped and reprobed using anti-β-*actin (*Sigma-Aldrich*). Bands were quantified in arbitrary units and normalized for protein concentrations using β-actin as loading control.

2.4.3.   Immunohistochemistry—Mice were treated with pentobarbital (75 mg kg^{-1}, IP) and sacrificed via cardiac exsanguination with phosphate-buffered saline (PBS, pH 7.4), followed by 4% paraformaldehyde. Brains were post-fixed for 2 h in 4% paraformaldehyde and transferred to 30% sucrose solution. Brains were snap frozen in ice-cold 2-methylbutane and stored at −20° C for further processing. Frozen sections were cut horizontally in 30-μm sections on a sliding microtome and collected into 0.01M phosphate buffered saline. For each brain, 7 to 8 equally spaced sections (approximately 270 μm apart) were collected through the orbitofrontal cortex. A series of adjacent sections was collected for cresyl echt violet staining. For immunohistochemical labeling of 5HT$_{2A}$ receptors, sections were incubated in blocking solution (10% normal goat serum [NGS] and 0.3% Triton X-100 in PBS) with 0.5% H$_2$O$_2$, followed by incubation in blocking solution alone. Sections were then incubated 48 h at 4° C in PBS containing 1% NGS, 0.3% Triton X-100, and a rabbit polyclonal antibody to the mouse 5-HT$_{2A}$ receptor (1:100, ImmunoStar, Hudson, WI, USA). Sections were rinsed in PBS and then incubated for 2 h in PBS containing 1% NGS, 0.3% Triton X-100, and biotinylated goat antirabbit IgG (1:200, Vector Laboratories, Burlingame, CA, USA). After rinsing in 0.3% Triton X- 100 in PBS (PBST), sections were incubated 1 h in PBST with ABC Complex (Vector Laboratories). Staining was visualized using a nickel intensified DAB reaction. After rinsing, sections were mounted on gelatin-subbed slides, dehydrated, cleared, and coverslipped. Control sections incubated without the primary antibody were generated and demonstrated no staining.

2.4.4.   Cortical Morphology—To examine potential strain differences in laminar morphology or soma size, two sections through the orbitofrontal cortex, matched for position along the dorsal-ventral axis, were chosen for morphological analyses. The medial-lateral boundaries of the orbitofrontal cortex are readily identifiable in cresyl echt violet-stained tissue, as are laminar boundaries, using standard cytoarchitectural criteria such as cell packing densities and laminar thicknesses. Using the StereoInvestigator system (MBF Bioscience, Williston, VT, USA) interfaced with a microscope (Nikon E80i, Nikon Instruments, Melville, NY, USA) via a video camera (Microfire, Optronics, Goleta, CA, USA), the thickness of each layer was measured at a final magnification of 1200x. To quantify soma area and volume, neurons were identified using standard morphological criteria (e.g., pale, multipolar soma and prominent nucleoli) and randomly sampled in an unbiased manner from layers II/III, V, and VI of the orbitofrontal cortex using StereoInvestigator's Fractionator probe. Soma area and volume were then estimated using the Nucleator probe at a final magnification of 1800x.

2.4.5.   Quantification of 5-HT$_{2A}$ receptor expression—5-HT$_{2A}$ receptor expression in the orbitofrontal cortex was quantified using a computer-based image analysis system (MCID, Interfocus Imaging, Cambridge, UK) interfaced with a microscope (Nikon E600, Nikon Instruments) via a monochrome video camera (Sony XC-ST70, Sony, Park Ridge, NJ, USA). Neurons were sampled from an 80 μm × 80 μm sampling frame at a final

magnification of 1980x. Ten sampling frames in both layers II-V and layer VI per animal were centered mediolaterally within the orbitofrontal cortex, and the sampling area size was chosen to yield approximately 7 neurons per frame. All labeled neurons contained within each sampling area were identified based on standard morphological criteria (large, multipolar soma) and the average relative optical density (ROD) per pixel of each soma was measured with values ranging from 0 (white) to 1 (black). To control for spurious differences in staining and illumination across sections and animals: 1) each round of staining contained animals from each group, 2) care was taken to minimize differences in illumination across samples, and 3) ROD measures within each section were expressed relative to white matter staining. ROD was measured in an area of white matter free of visible cell bodies in the corpus callosum directly below the orbitofrontal cortex. Relative intensity of neuronal staining was then calculated by dividing the ROD of each neuron by the ROD of the white matter in that section. This process was repeated in a portion of temporal-occipital cortex as a control. To assess differences in the distribution of staining intensities, 4-bin histograms of the mean number of neurons (expressed as percent of total) categorized as having relative intensities varying from more than 1.0 standard deviation below the mean of controls (low 5-HT_{2A}; very light) to within 1.0 standard deviation below the mean of controls (moderately low 5-HT_{2A}; light) to within 1.0 standard deviations above the mean of controls (moderately high 5-HT_{2A}; dark) to greater than 1.0 standard deviation above the mean (high 5-HT_{2A}; very dark) were generated. This method has been shown to be reliable for categorizing neurons by immunostaining intensity for subsequent frequency analyses and tends to be more sensitive to differences in protein expression assessed immunohistochemically than are simple means comparisons (Wilber *et al.,* 2009).

2.5. Statistical analyses

Normality and homoscedasticity were preliminarily verified using Kolmogorov-Smirnov and Bartlett's tests. Data were analyzed with one or multiway ANOVAs followed by Tukey's test for *post-hoc* comparisons, with Spjøtvoll-Stoline's correction for unequal n whenever necessary. Non-parametric data was analyzed using the Mann-Whitney and Kruskal-Wallis tests as appropriate, followed by Nemenyi's test for *post-hoc* assessment. Statistical analyses of developmental milestones were performed by Mantel-Cox log-rank test. Significance threshold was set at 0.05. All details of statistical analyses are indicated in the Supplementary Materials.

3. Results

3.1 Development of a mouse model of G×E interactions in ASB

To model the interaction between low-activity *Maoa* genotype and child maltreatment, *Maoa*^{Neo} hypomorphic mouse pups were subjected to a stressful regimen aimed at reproducing physical abuse and neglect. *Maoa* gene is located on the X chromosome; thus, HZ MAOA^{Neo} mothers were bred with WT males to obtain MAOA^{Neo} and WT littermate offspring. MAOA^{Neo} and WT pups were subjected to a daily regimen of either MS (mimicking neglect), SI (reproducing physical abuse) or their combination throughout the first three weeks of postnatal life, at different times and for variable durations each day (Fig. 1A). Unlike their WT littermates, MAOA^{Neo} pups exposed to both manipulations developed

a significant increase in aggression, as verified by their response towards foreign intruders on PND 80 (genotype × stress interaction, $F_{1,83}$=5.68, P = 0.02, 3-way ANOVA). Post-hoc analyses revealed that MAOA^{Neo} mice exposed to both stressors showed a significant enhancement in aggressive behaviors compared to MAOA^{Neo} mice exposed to MS or SI alone, or WT animals subjected to both or neither stressful manipulations (Ps < 0.001). Conversely, non-stressed WT and MAOA^{Neo} pups did not exhibit aggressive responses on PND 80, indicating that low MAOA activity (MAOA^{Neo} genotype) and early-life stress (MS + SI) are both necessary to elicit aggression in adult mice (Fig. 1B).

3.2 The first week of postnatal life is critical for G×E interactions to result in ASB-related responses

To narrow down the critical time window during which low-activity *Maoa* genotype interacts with the combination of MS and SI, we examined the impact of this stressful manipulation when limited to the first or the second postnatal week. MAOA^{Neo} mice exposed to this stressful schedule (hereafter designated as *G×E* mice) during the first, but not second postnatal week, exhibited greater aggression, as signified by a reduced latency to attack (H_5=25.98, P < 0.001, Kruskal-Wallis; Fig. 2A) and an increase in both the number of fighting episodes (genotype × time of stress interaction, $F_{2,84}$=16.28, P<0.00001, 2-way ANOVA; Fig. 2B) and overall fighting duration against unfamiliar WT mice in the home cage (genotype × time of stress interaction, $F_{2,84}$=13.21, P<0.00001, 2-way ANOVA; Fig. 2C). Notably, ES in the second postnatal week produced a reduction in aggressive responsiveness in WT, but not MAOA^{Neo} mice, as shown by a significant increase in latency to attack and decreases in the duration and number of attacks (Figs. 2A–C).

The analyses of social interaction with foreign conspecifics in an unfamiliar cage revealed that MAOA^{Neo} mice showed a genotype-specific reduction in overall social approaches (genotype × time of stress interaction, $F_{2,74}$=1.84, *NS;* main effect of genotype*: $F_{1,74}$*=5.97, P = 0.02; 2-way ANOVA; Fig. 2D) and duration (genotype × time of stress interaction: $F_{2,84}$=0.92, *NS;* Main effect of genotype*: $F_{1,74}$*=9.21, P = 0.003 2-way ANOVA; Fig. 2E); however, these deficits were not specifically affected by ES exposure, irrespective of its timing. Conversely, MAOA^{Neo} mice exposed to ES during the first, but not second postnatal week, reacted to social approaches initiated by the counterpart with a marked upsurge in asocial reactions (genotype × time of stress interaction: $F_{2,74}$=4.65, P = 0.01, 2-way ANOVA; Fig. 2F), due to a reduction in reciprocated approaches, combined with increases in escaping/withdrawing, freezing, offensive and attacking responses (Suppl. Table 1).

To ascertain that the behavioral abnormalities caused by stress during the first postnatal week may not reflect intrinsic abnormalities in the maternal behavior of HZ MAOA^{Neo} dams, we compared their responses to WT counterparts. Three-way, repeated-measure ANOVAs revealed that both WT and MAOA^{Neo} HZ mothers of stress-subjected pups spent more time engaged in pup care (environment × time interaction: $F_{1,31}$=29.96, P<0.00001; n= 8/group; Suppl. Fig. 1A) and active nursing (environment × time interaction: $F_{1,31}$=12.62, P = 0.00125; Suppl. Fig. 1B), but not passive nursing (environment × time interaction: $F_{1,31}$=1.94, *NS;* Suppl. Fig. 1C). This increase in active care was accompanied by a reduction in nest-building activities (environment × time interaction: $F_{1,31}$=8.27, P = 0.0072;

Suppl. Fig. 1D) and time spent off nest (environment × time interaction: $F_{1,31}$=4.84, P= 0.0353; Suppl. Fig. 1E), but not other maternal behaviors (environment × time interaction: $F_{1,31}$=0.51, *NS;* Suppl. Fig. 1F). Irrespective of the exposure of their pups to ES, no differences were found between genotypes, qualifying that WT and MAOA^{Neo} HZ mothers exhibit equivalent maternal behaviors.

3.3 Analysis of emotional domains and threat assessment in G×E mice

We then analyzed whether the ASB-related responses in *G×E* male mice subjected to ES during the first week of life may reflect other emotional alterations at PND 80 (Fig. 3). Behavioral analyses did not reveal significant interactions between genotype and stress with respect to locomotor activity (Total distance: genotype × stress interaction, $F_{1,35}$=0.12, *NS*; Time spent in the center of arena: genotype × stress interaction, $F_{1,35}$=0.96, *NS*; % Locomotor activity in the center of the arena: genotype × stress interaction, $F_{1,35}$=0.82, *NS*; 2-way ANOVA; Fig. 3A–D), startle reflex and PPI (Startle amplitude: genotype × stress interaction, $F_{1,33}$=0.63, *NS;* Prepulse inhibition: genotype × stress interaction, $F_{1,33}$=0.66, *NS*; 2-way ANOVA; Fig. 3E–F), spontaneous alternations (genotype × stress interaction: $F_{1,32}$=0.17, *NS*; 2-way ANOVA; Fig. 3G), light-dark box (genotype × stress interactions: $F_{1,27}$=1.71, *NS*; 2-way ANOVA; Fig. 3H), or novel-object exploration (Main effect of genotype: $F_{1,41}$=4.42, P= 0.04; 2-way ANOVA; Fig. 3I). However, MAOA^{Neo} mice exhibited significant reductions in total locomotor activity (Main effect of genotype: $F_{1,35}$=4.85, P= 0.03; Fig. 3B) and alterations (Main effect of genotype: $F_{1,32}$=4.87, P= 0.03; Fig. 3G), irrespective of ES exposure. The results of tail-suspension experiments showed that, while 80-day old, ES-exposed WT mice (designated as *E*) exhibited more immobility than their non-stressed counterparts (controls, designated as *CTL*), *G×E* mice displayed a significant reduction in these responses (genotype × stress interaction, $F_{1,69}$=6.51, P= 0.01; 2-way ANOVA; Fig. 3J) in comparison with unstressed MAOA^{Neo} mice (designated as *G*). To further assess the responsiveness of *G×E* mice towards acute stressors, they were tested in the predator-cued emergence paradigm (Fig. 3K–O). This task measures threat assessment by testing the propensity of mice to exit a secure enclosure and enter an arena with an anesthetized rat (Godar *et al.,* 2011) (Fig. 3K). In comparison with their controls, adult *G×E* males exhibited a greater tendency to enter the areas outside their enclosure and approach the rat (Fig. 3L), as signified by their reduced latency to enter the area occupied by the rat (H_3=14.07, P= 0.003; Kruskal-Wallis; Fig. 3M), as well as the longer time spent in this compartment (genotype × stress interaction: $F_{1,32}$=7.54, P= 0.01; 2-way ANOVA; Fig. 3N) and interacting with the rat itself (genotype × stress interaction $F_{1,32}$=4.18, P= 0.05; 2-way ANOVA; Fig. 3O).

3.4. Developmental trajectory of aggression in the G×E model.

Our next step was to verify the onset of behavioral aberrances in a new group of *G×E* male mice subjected to ES during the first week of life. Previous longitudinal studies in humans showed that the onset of violent conduct in individuals with low-activity *MAOA* genotype and history of child maltreatment occurs in adolescence (Fergusson *et al.*, 2011). In line with this idea, we tested home-cage aggressive responses in our model on PND 28 (7 days after weaning to enable familiarization with the new home-cage environment) and found that *G×E* mice attacked weight-matched intruders with a shorter latency and greater frequency

and duration (Latency to attack: H_1=24.17, P<0.00001; Kruskal-Wallis; Number of attacks: H_1=27.34, P<0.00001; Kruskal-Wallis; Attack duration: H_1=28.09, P<0.00001; Kruskal-Wallis; Number of social approaches: genotype × stress interaction : $F_{1,36}$=1.94, *NS;* 2-way ANOVA; Fig. 4A–C). When placed in an unfamiliar cage, mice exhibited no significant differences in social approaches towards a foreign conspecific (Number of social approaches: genotype × stress interaction : $F_{1,36}$=1.94, *NS*; Social interaction duration: $F_{1,36}$=2.29, *NS;* 2-way ANOVA; Fig. 4D–E). However, *G×E* mice displayed an augmentation of asocial responses in reaction to social approaches initiated by conspecifics (genotype × stress interaction: $F_{1,36}$=6.39, P = 0.02; 2-way ANOVA; Fig. 4F), due to a concomitant decrease of reciprocated reactions and increases of escaping/withdrawing, freezing, offensive and attacking responses (Suppl. Table 2). Consistently with our data in 80-day old *G×E* mice, alterations in social behaviors were not accompanied by specific changes in locomotion, exploration or anxiety-like responsiveness (Total distance: genotype × stress interactions for total distance: $F_{1,32}$=0.05, *NS*; Time in center: $F_{1,32}$=3.02, *NS*; 2-way ANOVA; %Locomotor activity: $F_{1,32}$=1.46, *NS*; 2-way ANOVA; Fig. 4H–J). However, adolescent MAOA^{Neo} mice showed a greater propensity to spend time in the light compartment of the light-dark box (Main effect of genotype: $F_{1,48}$=7.81, P = 0.007; genotype × stress interaction $F_{1,48}$=1.84, *NS*; 2-way ANOVA; Fig. 4K) and a lower proclivity to explore novel objects (Number of exploratory approaches: Main effect of genotype $F_{1,35}$=4.88, P = 0.03; genotype × stress interaction $F_{1,35}$=3.19, *NS;* Overall duration of exploration: Main effect of genotype $F_{1,35}$=4.23, P = 0.047; genotype × stress interaction $F_{1,35}$=1.03, *NS*; 2-way ANOVA; .Fig. 4L–M), irrespective of ES exposure.

3.5. Low resting heart rate is a premorbid marker of aggression in G×E mice.

One of the key clinical challenges posed by ASB prevention is the identification of premorbid signs or symptoms that may reliably predict future risk of psychopathology. Thus, we investigated whether *G×E* pups may display any neurobehavioral phenotypic alterations throughout ES or soon after its end (PND 8), which may serve as biomarkers of ASB vulnerability before the onset of aggressive manifestations. No significant *G×E* interactions were found for body weight (genotype × stress × time interaction: $F_{6,132}$=1.13; *NS*, 3-way ANOVA; Fig. 5A), even though both *G* and *G×E* mice displayed a slight, yet significant reduction in this parameter (genotype $F_{1,22}$=6.51, P = 0.02; 3-way ANOVA). A significant difference was detected in righting, but not geotaxis reflex throughout the first postnatal week (Righting reflex: X^2_{23}=35.84; P = 0.04; geotaxis reflex: X^2_{23}=1.81, *NS*; Mantel-Cox log-rank; Fig. 5B–C). Differences in righting reflex were found to reflect significant delays in *G*, *E* and *G×E* pups in comparison with non-stressed mice (Ps < 0.01); although the severity of this delay was more severe in *G×E* mice than *E* counterparts (P < 0.05), no differences between *G* and *G×E* mice were found.

Analyses of cortical morphology did not show any differences in cortical layer thickness or soma volume between groups on PND 8 (Thickness across different cortical layers: genotype × condition: $F_{1,23}$=4.01; *NS*; genotype × stress × layer interaction: $F_{2,46}$=1.32, *NS*; Soma volume: genotype × stress interaction: $F_{1,23}$=0.16, *NS*; genotype × stress × layer interaction: $F_{2,46}$=0.54, *NS*; 3-way ANOVA; Fig. 5D–H). In addition, no G×E interactions were identified in locomotor activity, although MAOA^{Neo} pups exhibited a greater activity

irrespective of their ES exposure (Total distance: Main effect of genotype: $F_{1,34}$=8.94, P = 0.005; genotype × stress interactions $F_{1,34}$=3.14, *NS;* Number of low-mobility bouts: Main effect of genotype $F_{1,34}$=14.78, P = 0.0005; genotype × stress interactions $F_{1,34}$=0.75, *NS;* Vertical force: Main effect of genotype: $F_{1,34}$=35.65, P<0.00001, genotype × stress interactions $F_{1,34}$=3.26, *NS*; 2-way ANOVA; Fig. 6A–D). Likewise, the analysis of ultrasonic vocalizations revealed a generalized reduction in communication in MAOA*Neo* mice, without any G×E interactions (Main effect of genotype: $F_{1,56}$=5.08, P = 0.03; genotype × stress interactions $F_{1,56}$=0.94, *NS*; 2-way ANOVA; Fig. 6E). Given that low-resting heart rate is the best-validated predictor of ASB in childhood and adolescence (Raine, 1990; Latvala *et al.,* 2015; Portnoy and Farrington, 2015), we also tested whether a similar characteristic may be present in 8-day old *G×E* pups. As shown in Fig.6F–G, these mice displayed a significant reduction in resting heart rate, as measured by an increase in the inter-beat interval [R-R; (genotype × stress interaction $F_{1,54}$=5.05, P = 0.03, 2-way ANOVA)]; this effect was not due to dysfunctions in heart dynamics, as indicated by the equivalent values of the ratio between other ECG intervals and the R-R duration (QRS/RR ratios: genotype × stress interaction $F_{1,54}$=0.001, *NS*; 2-way ANOVA; Fig. 6H).

3.6. G×E mice exhibit a selective increase in prefrontal 5-HT₂ₐ receptors.

Next, we studied the neurobiological mechanism of the interaction of early-life maltreatment and low-activity *MAOA* alleles. Given that the first postnatal week in mouse brain development is characterized by high 5-HT levels (Hohmann *et al.,* 1988), which play a key role in early cortical functioning (Rebello *et al.,* 2014), we hypothesized that the ontogeny of aggressive behavior in *G×E* mice may be underpinned by 5-HTergic alterations in this period. We first tested the levels of monoamines in *G×E* mice, as compared with the other groups. Both *G* and *G×E* pups displayed a dramatic elevation (approximately ten-fold) in forebrain 5-HT levels; however, no G×E differences were detected (Main effect of genotype: $F_{1,28}$=633.9, P<0.00001; genotype × stress interactions $F_{1,28}$=0.10, *NS*; 2-way ANOVA; Fig. 7A). A milder (~30–40%), yet significant increase in norepinephrine levels was also found in both *G* and *G×E* mice (Main effect of genotype: $F_{1,28}$=67.66, P<0.00001; genotype × stress interactions $F_{1,28}$=4.66, *NS;* 2-way ANOVA; Fig. 7B), without any significant difference between these two groups. Finally, no significant differences were found for dopamine levels (genotype × stress interaction $F_{1,24}$=0.05, *NS*; 2-way ANOVA; Fig. 7C).

Given the dramatic enhancement in 5-HT observed in both *G* and *G×E* pups, we hypothesized that the selective effects of stress on MAOA*Neo* mice may be due to selective alterations in the expression of the receptors for this neurotransmitter. Western-blot analyses of 5-HT receptor expression in the PFC revealed no differences for 5-HT₁ₐ (genotype × stress interaction: $F_{1,16}$=0.32, *NS*; 2-way ANOVA; Fig. 7D), 5-HT₁B (genotype × stress interaction $F_{1,16}$ =0.14, *NS*; 2-way ANOVA; Fig. 7E), and 5-HT₂C (genotype × stress interaction $F_{1,16}$=0.001; *NS*; 2-way ANOVA; Fig. 7F); conversely, 5-HT₂ₐ levels were significantly enhanced in *G×E* mice (genotype × stress interaction $F_{1,20}$=4.46, P = 0.047; 2-way ANOVA; Fig. 7G). Immunohistochemical studies revealed that these changes were particularly pronounced in the orbitofrontal cortex (genotype × stress × stain intensity interaction $F_{3,78}$=3.55, P = 0.02; 3-way ANOVA; Fig. 8A–B); conversely, no differences

were found in the temporal-occipital cortex (genotype × stress × stain intensity interaction $F_{3,66}$=1.22, *NS*; 3-way ANOVA; Fig. 8C–D).

3.7.   Antagonism of 5-HT$_{2A}$ receptors throughout the first postnatal week rescues ASB-related phenotypes in GxE mice.

To test whether 5-HT$_{2A}$ receptors may mediate the interaction of low-activity *Maoa* genotype and early-life stress, we treated *G×E* pups daily with the 5-HT$_2$ receptor blocker ketanserin (KET, 1–3 mg kg^{-1}/day, IP) and the selective 5-HT$_{2A}$ receptor antagonist MDL (0.1–0.3 mg kg^{-1}/day, IP) throughout the first postnatal week.

As shown in Fig. 9(A–C), KET significantly reduced the propensity of *G×E* mice to attack their counterparts, and surprisingly increased the overall duration of the attacks initiated by *E* resident mice, without significantly affecting their latency and number (Latency to attack: genotype × treatment interactions $F_{2,54}$=5.51, *P* = 0.007; Number of attacks: genotype × treatment interactions $F_{2,54}$=11.41, *P* = 0.00007; Overall attack duration: genotype × treatment interactions $F_{2,54}$=11.58, *P* = 0.00007; 2-way ANOVA; Fig. 9A–C). In an unfamiliar cage, KET-treated *G×E* mice exhibited greater overall duration (genotype × treatment interactions $F_{2,42}$=14.02, *P* = 0.00002; 2-way ANOVA) and number of social approaches (genotype × treatment interactions $F_{2,42}$=12.13, *P* = 0.00007; 2-way ANOVA; Fig. 9D–E), as well as greater reduction in non-reciprocal responses in *G×E* mice (genotype × treatment interactions $F_{2,42}$=8.42, *P* = 0.0008; 2-way ANOVA; Fig. 9F and Suppl. Table 3). Conversely, KET did not produce any significant effects in the behavior of *E* mice.

In keeping with these findings, MDL dose-dependently rescued aggressive behaviors in *G×E* animals, while increasing the number and duration of attacks initiated by *E* littermates (Latency to attack: genotype × treatment interactions $F_{2,42}$=10.19, *P* = 0.003; number of attacks: genotype × treatment interactions $F_{2,42}$=12.42, *P* = 0.0006; overall attack duration: genotype × treatment interactions $F_{2,42}$=13.61, *P* = 0.00003; 2-way ANOVA; Fig. 10A–C). The same compound increased the duration (genotype × treatment interactions $F_{2,42}$=3.31, *P* = 0.046; 2-way ANOVA; Fig. 10D), but not the number of social approaches (genotype × treatment interactions $F_{2,42}$=0.53, *NS*; 2-way ANOVA; Fig. 10E) initiated by *G×E* mice. Finally, MDL-treated *G×E* mice increased the reciprocation of social approaches and decreased non-reciprocal reactions, including withdrawing, offensive and attacking responses (% Asocial responsiveness: genotype × treatment interactions $F_{2,42}$=3.84, *P* = 0.03; 2-way ANOVA; Fig. 10E and Suppl. Table 4).

Further analyses of the effects of 5-HT$_{2A}$ receptor blockade during early life revealed other specific phenotypic alterations in *G×E* animals. In particular, MDL administration in the first postnatal week normalized resting bradycardia in *G×E* pups at PND 8 (interbeat interval: $F_{1,15}$=13.93, *P* = 0.002; 1-way ANOVA; Suppl. Fig. 2A–B) without altering overall heart rate dynamics (QRS/RR ratio: $F_{1,15}$=0.84, *NS*; 1-way ANOVA; Suppl. Fig. 2C).

Discussion

In the present study, we developed the first mouse model of the best-established G×E interaction in ASB, by subjecting MAOA^{Neo} pups to MS and SI throughout the first

postnatal week. This manipulation elicited aggressive responses, as well as overt deficits in the reciprocation of social approaches in adolescent and adult MAOA^{Neo}, but not WT, males. Both these behavioral responses and their developmental trajectory bear a striking resemblance with the pathognomonic clinical phenotypes of ASB. The high face validity of this model is also supported by additional findings: first, MAOA^{Neo} mice exposed to ES exhibited abnormal stress reactivity and poor threat assessment, two characteristics commonly observed in the ASB spectrum (Blair, 1999; Loney *et al.,* 2006; Fairchild *et al.,* 2008; von Borries *et al.,* 2012); second, the onset of aggression in *G×E* mice occurs in adolescence, in striking resemblance with the developmental trajectory described for G×E interactions in ASB (Fergusson *et al.,* 2011); third, G×E mice displayed a significant reduction in resting heart rate, a well-established biomarker of ASB susceptibility in children and adolescents (Raine, 1990; Latvala *et al.,* 2015; Portnoy and Farrington, 2015). Aside from the heuristic value of our model as an experimental tool to study the neurodevelopmental trajectory of ASB, these findings provide the first experimental validation of G×E interactions in aggression and other ASB-related traits. Such interactions, to date, have exclusively been supported by observational studies, and sometimes challenged by contrasting evidence (Haberstick *et al.,* 2014).

The optimal conditions that elicited aggression in MAOA^{Neo} mice were based on a pseudorandom sequence of daily sessions of MS and SI; both stressors were administered at various times of the day and with variable durations during the first postnatal week. Conversely, neither stressor alone produced any significant enhancement in aggression in MAOA^{Neo} mice, suggesting that multidimensional schedules of early-life chronic, uncontrollable stress may be better suited to trigger enduring behavioral outcomes. Additionally, this finding lends support to the concept that the severity of the long-term sequelae of early-life maltreatment may be best related to the cumulative burden of abuse and neglect (Dong *et al.,* 2004; Anda *et al.,* 2006), rather than to the impact of single stressors.

The specificity of the first postnatal week for G×E interactions in our model points to this developmental stage as a key time window for the ontogeny of ASB-related phenotypes. While traditional models of development have equated the first week of postnatal development in rodents to the third trimester of gestational development in humans, comparative timescales of maturational ages between species vary depending on the specific benchmark (Semple *et al.,* 2013). From this perspective, it is worth noticing that the first week of postnatal life in mice is characterized by a prominent increase in 5-HT levels (Hohmann *et al.,* 1988). In the human brain, comparable increases in 5-HT content occur during the first 2–5 years of life (Hedner *et al.,* 1986); however, given the key role of *MAOA* in conditioning cortical 5-HT levels in early developmental stages (Cases *et al.,* 1995), the elevation in the concentrations in this neurotransmitter in humans may be prolonged in carriers of low-activity *MAOA* genotype. Irrespective of this issue, these data confirm prior evidence pointing to early life as a period of high vulnerability for the interplay of heritable and contextual influences in the ontogeny of ASB (Caspi *et al.,* 2002; Fergusson *et al.,* 2011). Future studies will be needed to assess whether the ES schedule applied to our model may reflect the impact of stress during fetal development rather than in early childhood.

The aggression and social reciprocation deficits observed in *G×E* mice were not accompanied by overt changes in perception, working memory, exploration or anxiety-like responses; however, we observed a reduction in stress-induced immobility in the tail suspension paradigm, as well as threat assessment in the predator-cued emergence task. These features strongly suggest that the interaction of low-activity *MAOA* and early-life maltreatment may progressively lower stress reactivity and threat sensitivity. One of the key psychobiological frameworks to understand ASB posits that the exposure to high levels of violence in early life may lead to a desensitization of stress response and threat reactivity, ultimately resulting in a greater proclivity to ASB (Mrug *et al.*, 2016). In keeping with our previous characterizations (Bortolato *et al.*, 2011), MAOA^{Neo} mice displayed a marked reduction in social interaction, irrespective of ES exposure and timing. These findings suggest that, although *MAOA* deficiency is associated with greater risk for both social deficits and aggression, these two domains likely reflect partially divergent neurobiological substrates. From this perspective, the social exploration deficits in MAOA^{Neo} mice may reflect a generalized reduction in their exploratory drive, as shown by the lower novel-object exploration duration (Figs. 3 and 5).

In contrast with *G×E* littermates, *E* mice exhibited a significant increase in tail-suspension immobility – a response typically interpreted as reflective of behavioral despair in the validation of antidepressants (Castagné *et al.*, 2011). Given that high-activity *MAOA* variants have been highlighted as a predisposing factor for depression (Dannlowski *et al.*, 2009), our results may suggest a role of *MAOA* in the moderation of different psychopathological outcomes of early-life stress, including depressive symptoms. While this idea was beyond the scope of the present work, future studies are warranted to further explore this issue with animal models that can better capture the ontogeny and manifestations of depression.

In comparison with their controls, *G×E* pups were found to display lower resting heart rate; notably, in children this sign is regarded as one of the most robust predictors of ASB and violence (Raine, 1990; Portnoy and Farrington, 2015). To the best of our knowledge, *G×E* mice are the first animal models reproducing phenotypes related to ASB during a developmental stage prior to the onset of aggression. Resting bradycardia is associated with low autonomic arousal and reflects a reduction in noradrenergic function and/or increased vagal tone; however, the causes of this sign in ASB remain unclear (Scarpa *et al.*, 2008). Thus, from this perspective, our model may prove extremely interesting to investigate the neurobiological basis of this phenotype.

We documented that, irrespective of ES exposure, MAOA^{Neo} pups exhibited a significant reduction in body weight, delayed acquisition of righting reflex, hyperactivity, and reduced vocalizations. These phenotypes are highly reminiscent of the deficits observed in MAOA knockout pups (Cases *et al.*, 1995; Bortolato *et al.*, 2013a), further highlighting the importance of this enzyme in early developmental stages. According, recent clinical evidence has shown developmental delays in boys harboring nonsense *MAOA* mutations (Bortolato *et al.*, 2018). Interestingly, antisocial and externalizing tendencies in children are associated with hyperactivity (Barkley et al., 2004), low body weight (Cimino et al., 2016), and communication deficits (Petersen et al., 2013); in view of this background, our findings

raise the intriguing possibility that these associations may be moderated by low-activity MAOA alleles.

MAOA^{Neo} pups showed increased forebrain levels of 5-HT, and, to a lesser extent, norepinephrine, but not dopamine. These data are in agreement with prior evidence showing that, in mice, MAOA primarily catalyzes the degradation of 5-HT and norepinephrine, but not dopamine (plausibly due to the actions of MAOB and COMT on the latter neurotransmitter) (Bortolato *et al.*, 2008). Furthermore, these findings are aligned to previous results showing that MAOA knockout pups during the first postnatal week feature extremely high levels of brain 5-HT, with much more modest elevations in catecholamines levels (Cases *et al.*, 1995). Indeed, MAOA^{Neo} mice exhibit very low levels of enzyme in the brain, leading to a marked elevation of 5-HT, and a much more modest increase in norepinephrine (Bortolato *et al.*, 2011). Interestingly, ES did not affect the forebrain content of these neurotransmitters either in WT and MAOA^{Neo} mice, indicating that this environmental manipulation during the first postnatal week is unlikely to significantly alter either monoamine synthesis or metabolism.

Our results revealed that G×E interaction led to a significant up-regulation of 5-HT$_{2A}$ receptors in the PFC during the first week of postnatal life. These results are in line with previous evidence indicating that ES leads to a selective up-regulation and activation of these receptors in the PFC (Benekareddy et al, 2010; Sood et al., 2018). In rodents, 5-HT$_{2A}$ receptor density in the brain is relatively low in the perinatal period, and estimated to reach only ~20% of the levels observed in adults (Roth, 1991); however, the expression of these receptors increases progressively from P3 through the first three postnatal weeks (Li *et al.*, 2004), and their activation in this period – and particularly at its beginning - is posited to promote the activation of pyramidal cells of the PFC (Beique *et al.*, 2004). Of note, 5-HT$_{2A}$ receptor antagonism during the first postnatal week attenuated aggression in GxE mice (as well as resting bradycardia in pups). The most direct interpretation of these findings is that activation of 5-HT$_{2A}$ receptors in the PFC may mediate the ontogeny of aggression in *G×E* mice. However, a final demonstration of this idea will require future analyses with viral vectors and/or other constructs that may help reduce 5-HT$_{2A}$ receptor activity selectively in the PFC during the first postnatal week.

These results extend previous evidence indicating that both KET and MDL dose-dependently reduced aggression in adult MAOA knockout mice, pointing to the possibility that the activation of prefrontal 5-HT$_{2A}$ receptors may be critical to mediate the impact of MAOA deficiency on aggression (Shih et al., 1999), also with respect to its interaction with ES. As 5-HT$_{2A}$ receptors modulate the function of the corticolimbic circuitry that regulates affective reactivity (Beique *et al.,* 2007), it is possible that their activation in early-life may lead to alterations in the organization of the PFC, in turn leading to threat assessment deficits and negative bias towards social cues.

To our surprise, we also found that both MDL and KET dose-dependently enhanced the likelihood of aggressive responses in resident WT mice. While the mechanisms whereby early-life antagonism of 5-HT$_{2A}$ receptors facilitates the emergence of aggression in ES-exposed mice remain elusive, our data suggest that the activation of this receptor may be

critical to offset the long-term outcomes of ES. In line with this interpretation, early-life KET treatment has been shown to prevent the increase in anxiety-related outcomes following ES (Benekareddy *et al.*, 2011). This background suggests that 5-HT$_{2A}$ receptor antagonism during the first week may increase the aggressive reactivity of resident *E* mice by reducing their anxiety-like behaviors. In potential support of this idea, neither KET nor MDL significantly altered E mice's latency to attack, a parameter that may reflect aspects of aggression more directly related to impulsivity. Further studies will verify this hypothesis by evaluating how 5-HT$_{2A}$ antagonism modifies anxiety-like and stress responsiveness in *E* and *GxE* mice. Independently from the mechanisms underpinning the bidirectional outcomes of 5-HT$_{2A}$ receptor blockade with respect to aggression, our results collectively suggest that early-life 5-HT$_{2A}$ receptor antagonism may either increase or decrease the risk of aggressive conduct, depending on their genetic profile.

Given the importance of 5-HT$_{2A}$ receptors in remodeling of spines and dendrites in the pyramidal neurons, as well as in the functional modulation of the corticolimbic circuitry regulating affective reactivity (Beique *et al.,* 2007), early-life 5-HT$_{2A}$ receptor stimulation may lead to threat assessment deficits and negative cognitive bias towards social and affective cues. In turn, these changes may promote aggression in later developmental stages (Aznar and Klein, 2013), possibly in relation to additional factors such as increases in dopamine release in the nucleus accumbens (Yu *et al.,* 2014). Notably, 5-HT$_{2A}$ receptors have been shown to play a key role in shaping HPA response to stress (Bagdi *et al.,* 1996) and dopaminergic activity (Bortolozzi *et al.,* 2005). Intriguingly, dopamine release in the nucleus accumbens during adolescence has been shown to be critical in mediating aggressive behavior in MAOA mutants (Magalhaes *et al.,* 2010). Previous studies have shown that, in mice, MAOA catabolizes dopamine predominantly in juvenile stages (Bortolozzi *et al.,* 2005). Taken together, these results may indicate that the role of MAOA may follow a "two-hit" developmental model, according to which hypoactivity of this enzyme in early life would interact with chronic stress to result in the activation of 5-HT$_{2A}$ receptor, and this predisposition would in change predispose both HPA and catecholaminergic responses to stress, which would become essential for ASB pathogenesis from adolescence onwards. Future studies will need to confirm this intriguing pathophysiological framework and evaluate the long-term sequelae of early 5-HT$_{2A}$ receptor activation on HPA and catecholaminergic responses to social cues.

The mechanisms whereby the total amount of 5-HT$_{2A}$ receptors in the prefrontal cortex are upregulated only in G×E mice remain elusive. An intriguing hypothesis, which will need to be investigated in future studies, is that changes in this receptor may reflect alterations in the trafficking of 5-HT$_{2A}$ receptors, in turn stimulated by stress-mediated activation of CRF$_1$ receptors (Magalhaes *et al.,* 2010). Understanding the process that leads to a selective upregulation of 5-HT$_{2A}$ receptors in early life in response to stress will be critical to identify the actual mechanistic bases of this G×E interaction.

Several open questions also remain on the phenomenological significance of the G×E interactions in our model. The main mechanistic framework to account for G×E interactions in psychopathology is the *diathesis-stress model*, which posits the synergistic convergence of genetic and environmental factors across critical early developmental periods to predispose

to specific neurobehavioral and cognitive deficits (Zuckerman, 1999). An alternative conceptualization of the G×E interactions in ASB may follow the *differential susceptibility* model, which postulates that genetic proneness accounts for sensitivity to both unfavorable and supportive environments (Ellis *et al.,* 2011). In line with this hypothesis, emerging evidence has pointed to the possibility that low-activity *MAOA* variants may serve as "plasticity alleles" that may confer differential susceptibility to substance use depending on the rearing environment (Belsky *et al.,* 2011). If this conceptualization were applicable to our model, environmental enrichments in early-life stages may lead to a reduction of aggressive tendencies in adolescence and adulthood. While some authors have proposed that early-life handling may lead to long-term beneficial effects (Fernandez-Teruel *et al.,* 2002), it may be argued that this type of manipulation during the first week of postnatal life may interfere with maternal care and result in enduring detrimental outcomes. Future research is needed to determine what type of interventions may qualify as environmental enrichment at such an early life stage, and ultimately define which theoretical model may best predict the phenotypic outcomes in our G×E model.

Several limitations of this study should be acknowledged. First, this study focused exclusively on male mice; while the higher frequency of early traumas in girls points to the relevance of our paradigm to females, the scope of this study was to define the optimal conditions to model GxE interactions in ASB, which have been best demonstrated in males. Future studies, however, will be dedicated to the analysis of ES in female MAOA^{Neo} mice. Second, although our model recapitulates GxE interactions in ASB and exhibits several responses related to this condition, caution should be advocated against the risk of anthropomorphic bias in the interpretation of our findings. Indeed, ASB encompasses several behavioral features that cannot be accurately captured in an animal model, such as the lack of social norms, lack of responsibility and deceitfulness. These limitations notwithstanding, our model appears to have unique translational advantages, which may prove critical to refine our understanding of some of the neurobiological and developmental bases of ASB and help develop novel and better therapeutic interventions for this staggering condition.

Supplementary Material

Refer to Web version on PubMed Central for supplementary material.

Acknowledgements:

Abbreviations:

ASB	antisocial behavior
ES	early-life stress

5-HT	serotonin
G × E	gene by environment
HZ	heterozygous
IP	intraperitoneal injection
MAOA	monoamine oxidase A
MAOA ^{Neo}	MAO-A hypomorphic mice
MS	Maternal separation
NGS	normal goat serum
PFC	prefrontal cortex
PPI	prepulse inhibition of the startle reflex
PND	postnatal day
ROD	relative optical density
R-R	inter-beat interval
SI	Saline intraperitoneal injections
VNTR	variable tandem repeat
WT	wild type

References

Anda RF, Felitti VJ, Bremner JD, Walker JD, Whitfield C, Perry BD, Dube SR, Giles WH 2006 The enduring effects of abuse and related adverse experiences in childhood. European archives of psychiatry and clinical neuroscience 256(3), 174–186. [PubMed: 16311898]

Aznar S, Klein AB 2013 Regulating prefrontal cortex activation: an emerging role for the 5-HT$_2$A serotonin receptor in the modulation of emotion-based actions? Mol Neurobiol. 48, 841–53. [PubMed: 23696058]

Bagdy G. 1996 Role of the hypothalamic paraventricular nucleus in 5-HT1A, 5-HT2A and 5-HT2C receptor-mediated oxytocin, prolactin and ACTH/corticosterone responses. Behav Brain Res. 73(1–2), 277–80. [PubMed: 8788518]

Barkley RA, Fischer M, Smallish L, Fletcher K. 2004 Young adult follow-up of hyperactive children: antisocial activities and drug use. J Child Psychol Psychiatry. 45, 195–211. [PubMed: 14982236]

Béïque JC, Campbell B, Perring P, Hamblin MW, Walker P, Mladenovic L, Andrade R. 2004 Serotonergic regulation of membrane potential in developing rat prefrontal cortex: coordinated expression of 5-hydroxytryptamine (5-HT)1A, 5-HT2A, and 5-HT7 receptors. J Neurosci. 24, 4807–4817. [PubMed: 15152041]

Béïque JC, Imad M, Mladenovic L, Gingrich JA, Andrad R. 2007 Mechanism of the 5-hydroxytryptamine 2A receptor-mediated facilitation of synaptic activity in prefrontal cortex. Proc Natl Acad Sci. 104, 9870–9875. [PubMed: 17535909]

Belsky J, Beaver KM 2011 Cumulative-genetic plasticity, parenting and adolescent self-regulation. J Child Psychol Psychiatry 52, 619–626. [PubMed: 21039487]

Benekareddy M, Goodfellow NM, Lambe EK, Vaidya VA 2010 Enhanced function of prefrontal serotonin 5-HT(2) receptors in a rat model of psychiatric vulnerability. J Neurosci. 30, 12138–12150.

Benekareddy M, Vadodaria KC, Nair AR, Vaidya VA 2011 Postnatal serotonin type 2 receptor blockade prevents the emergence of anxiety behavior, dysregulated stress-induced immediate early gene responses, and specific transcriptional changes that arise following early life stress. Biol Psychiatry. 70, 1024–1032. [PubMed: 21959103]

Blair RJ 1999 Responsiveness to distress cues in the child with psychopathic tendencies. Pers Ind Diff. 27, 135–145.

Bortolato M, Chen K, Godar SC, Chen G, Wu W, Rebrin I, Farrell MR, Scott AL, Wellman CL, Shih JC 2011 Social deficits and perseverative behaviors, but not overt aggression, in MAO-A hypomorphic mice. Neuropsychopharmacology 36, 2674–2688. [PubMed: 21832987]

Bortolato M, Chen K, Shih JC 2008 Monoamine oxidase inactivation: from pathophysiology to therapeutics. Adv Drug Deliv Rev. 60, 1527–1533. [PubMed: 18652859]

Bortolato M, Floris G, Shih JC 2018 From aggression to autism: new perspectives on the behavioral sequelae of monoamine oxidase deficiency. J Neural Transm. 125, 1589–1599. [PubMed: 29748850]

Bortolato M, Godar SC, Alzghoul L, Zhang J, Darling RD, Simpson KL, Bini V, Chen K, Wellman CL, Lin RC, Shih JC 2013a Monoamine oxidase A and A/B knockout mice display autistic-like features. Int J Neuropsychopharmacol. 16, 869–888. [PubMed: 22850464]

Bortolato M, Yardley MM, Khoja S, Godar SC, Asatryan L, Finn DA, Alkana RL, Louie SG, Davies DL 2013b Pharmacological insights into the role of P2X4 receptors in behavioural regulation: lessons from ivermectin. Int J Neuropsychopharmacol. 16(5), 1059–1070. [PubMed: 23174033]

Bortolozzi A, Díaz-Mataix L, Scorza MC, Celada P, Artigas F. 2005 The activation of 5-HT receptors in prefrontal cortex enhances dopaminergic activity. J Neurochem. 95(6), 1597–1607. [PubMed: 16277612]

Byrd AL, Manuck SB 2014 MAOA, childhood maltreatment, and antisocial behavior: meta-analysis of a gene-environment interaction. Biol Psychiatry 75, 9–17. [PubMed: 23786983]

Cases O, Seif I, Grimsby J, Gaspar P, Chen K, Pournin S, Müller U, Aquet M, Babinet C, Shih JC, De Maeyer E. 1995 Aggressive behavior and altered amounts of brain serotonin and norepinephrine in mice lacking MAOA. Science 268(5218), 1763–1766. [PubMed: 7792602]

Caspi A, McClay J, Moffitt TE, Mill J, Martin J, Craig IW, Taylor A, Poulton R. 2002 Role of genotype in the cycle of violence in maltreated children. Science 297, 851–854. [PubMed: 12161658]

Castagné V, Moser P, Roux S, Porsolt RD 2011 Rodent models of depression: forced swim and tail suspension behavioral despair tests in rats and mice. Curr Protoc Neurosci. Chapter 8: Unit 8.10A.

Chu V, Otero JM, Lopez O, Morgan JP, Amende I, Hampton TG 2001 Method for non-invasively recording electrocardiograms in conscious mice. BMC Physiol. 1, 6. [PubMed: 11476671]

Cimino S, Cerniglia L, Almenara CA, Jezek S, Erriu M, Tambelli R. 2016 Developmental trajectories of body mass index and emotional-behavioral functioning of underweight children: A longitudinal study. Sci Rep. 6, 20211.

Compton WM, Conway KP, Stinson FS, Colliver JD, Grant BF 2005 Prevalence, correlates, and comorbidity of DSM-IV antisocial personality syndromes and alcohol and specific drug use disorders in the United States: results from the national epidemiologic survey on alcohol and related conditions. J Clin Psychiatry 66, 677–685. [PubMed: 15960559]

Dannlowski U, Ohrmann P, Konrad C, Domschke K, Bauer J, Kugel H, Hohoff C, Schoning S, Kersting A, Baune BT, Mortensen LS, Arolt V, Zwitserlood P, Deckert J, Heindel W, Suslow T. 2009 Reduced amygdala-prefrontal coupling in major depression: association with MAOA genotype and illness severity. Int J Neuropsychopharmacol. 12(1), 11–22. [PubMed: 18544183]

Dong M, Anda RF, Felitti VJ, Dube SR, Williamson DF, Thompson TJ, Loo CM, Giles WH 2004 The interrelatedness of multiple forms of childhood abuse, neglect, and household dysfunction. Child abuse & neglect. 28(7), 771–784. [PubMed: 15261471]

Ellis BJ, Boyce WT, Belsky J, Bakermans-Kranenburg MJ, van Ijzendoorn MH 2011 Differential susceptibility to the environment: an evolutionary--neurodevelopmental theory. Dev Psychopathol. 23, 7–28. [PubMed: 21262036]

Fairchild G, van Goozen SH, Stollery SJ, Brown J, Gardiner J, Herbert J, Goodyer IM 2008 Cortisol diurnal rhythm and stress reactivity in male adolescents with early-onset or adolescence-onset conduct disorder. Biol Psychiatry. 64(7), 599–606. [PubMed: 18620338]

Fava M. 1997 Psychopharmacologic treatment of pathologic aggression. Psychiatr Clin North Am. 20(2), 427–451. [PubMed: 9196923]

Fergusson DM, Boden JM, Horwood LJ, Miller AL, Kennedy MA 2011 MAOA, abuse exposure and antisocial behavior: 30-year longitudinal study. Br J Psychiatry 198, 457–463. [PubMed: 21628708]

Fernández-Teruel A, Giménez-Llort L, Escorihuela RM, Gil L, Aguilar R, Steimer T, Tobeña A. 2002 Early-life handling stimulation and environmental enrichment: are some of their effects mediated by similar neural mechanisms? Pharmacol Biochem Behav. 73(1):233–245. [PubMed: 12076742]

Fowler SC, Birkestrand BR, Chen R, Moss SJ, Vorontsova E, Wang G, Zarcone TJ 2001 A force-plate actometer for quantitating rodent behaviors: illustrative data on locomotion, rotation, spatial patterning, stereotypies, and tremor. J Neurosci Methods 107, 107–124. [PubMed: 11389948]

Godar SC, Bortolato M, Frau R, Dousti M, Chen K, Shih JC 2011 Maladaptive defensive behaviours in monoamine oxidase A-deficient mice. Int J Neuropsychopharmacol. 14, 1195–1207. [PubMed: 21156093]

Godar SC, Fite PJ, McFarlin KM, Bortolato M. 2016 The role of monoamine oxidase A in aggression: current translational developments and future directions. Prog Neuropsychopharmacol Biol Psychiatry 269, 90–100.

Grappi S, Marchese G, Secci ME, De Montis MG, Gambarana C, Scheggi S. 2011 Morphine sensitization as a model of mania: comparative study of the effects of repeated lithium or carbamazepine administration. Pharmacol Biochem Behav. 99(4), 749–758. [PubMed: 21741986]

Haberstick BC, Lessem JM, Hewitt JK, Smolen A, Hopfer CJ, Halpern CT, Killeya-Jones LA, Boardman JD, Tabor J, Siegler IC, Williams RB, Mullan Harris K. 2014 MAOA genotype, childhood maltreatment, and their interaction in the etiology of adult antisocial behaviors. Biol Psychiatry 75(1), 25–30. [PubMed: 23726513]

Hedner J, Lundell KH, Breese GR, Mueller RA, Hedner T. 1986 Developmental variations in CSF monoamine metabolites during childhood. Biol Neonate 49(4), 190–197. [PubMed: 2423144]

Heyser CJ. Assessment of developmental milestones in rodents (2003). Curr Protoc Neurosci. Supp 25.

Hohmann CF, Hamon R, Batshaw ML, Coyle JT 1988 Transient postnatal elevation of serotonin levels in the mouse neocortex. Dev Brain Res. 43, 163–166.

Kehne JH, Baron BM, Carr AA, Chaney SF, Elands J, Feldman DJ, Frank RA, van Giersbergen PL, McCloskey TC, Johnson MP, McCarty DR, Poirot M, Senyah Y, Siegel BW, Widmaier C. 1996 Preclinical characterization of the potential of the putative atypical antipsychotic MDL 100,907 as a potent 5-HT2A antagonist with a favorable CNS safety profile. J Pharmacol Exp Ther. 277, 968–981. [PubMed: 8627580]

Khalifa N, Duggan C, Stoffers J, Huband N, Völlm BA, Ferriter M, Lieb K. 2010 Pharmacological interventions for antisocial personality disorder. Cochrane Database Syst Rev.8: CD007667.

Kim-Cohen J, Caspi A, Taylor A, Williams B, Newcombe R, Craig IW, Moffitt TE 2006 MAOA, maltreatment, and gene-environment interaction predicting children's mental health: new evidence and a meta-analysis. Mol Psychiatry 11, 903–913. [PubMed: 16801953]

Latvala A, Kuja-Halkola R, Almqvist C, Larsson H, Lichtenstein P. 2015 A longitudinal study of resting heart rate and violent criminality in more than 700000 men. JAMA Psychiatry 72, 971–978. [PubMed: 26351735]

Leysen JE, Awouters F, Kennis L, Laduron PM, Vandenberk J, Janssen PA 1981 Receptor binding profile of R 41 468, a novel antagonist at 5-HT2 receptors. Life Sci 28, 1015–1022. [PubMed: 6261070]

Li QH, Nakadate K, Tanaka-Nakadate S, Nakatsuka D, Cui Y, Watanabe Y. 2004 Unique expression patterns of 5-HT2A and 5-HT2C receptors in the rat brain during postnatal development: Western blot and immunohistochemical analyses. J Comp Neurol. 469, 128–140. [PubMed: 14689478]

Loney BR, Butler MA, Lima EN, Counts CA, Eckel LA 2006 The relation between salivary cortisol, callous-unemotional traits, and conduct problems in an adolescent non-referred sample. J Child Psychol Psychiatry 47(1), 30–36. [PubMed: 16405638]

Magalhaes AC, Holmes KD, Dale LB, Comps-Agrar L, Lee D, Yadav PN, Drysdale L, Poulter MO, Roth BL, Pin JP, Anisman H, Ferguson SS 2010 CRF receptor 1 regulates anxiety behavior via sensitization of 5-HT2 receptor signaling. Nat Neurosci. 13, 622–629. [PubMed: 20383137]

Mrug S, Madan A, Windle M. 2016 Emotional desensitization to violence contributes to adolescents' violent behavior. Journal Abnorm Child Psychol. 44, 75–86.

Petersen IT, Bates JE, D'Onofrio BM, Coyne CA, Lansford JE, Dodge KA, Pettit GS, Van Hulle CA 2013 Language ability predicts the development of behavior problems in children. J Abnorm Psychol. 122, 542–557. [PubMed: 23713507]

Portnoy J, Farrington DP 2015 Resting heart rate and antisocial behavior: An updated systematic review and meta-analysis. Aggress Viol Behav. 22, 33–45.

Raine A. 2002 Biosocial studies of antisocial and violent behavior in children and adults: a review. J Abnorm Child Psychol. 30, 311–326. [PubMed: 12108763]

Raine A, Venables PH, Williams M. 1990 Relationships between central and autonomic measures of arousal at age 15 years and criminality at age 24 years. Arch Gen Psychiatry 47, 1003–1007. [PubMed: 2241502]

Rebello TJ, Yu Q, Goodfellow NM, Caffrey Cagliostro MK, Teissier A, Morelli E, Demireva EY, Chemiakine A, Rosoklija GB, Dwork AJ, Lambe EK, Ginqrich JA, Ansorge MS 2014 Postnatal day 2 to 11 constitutes a 5-HT-sensitive period impacting adult mPFC function. J Neurosci. 34, 12379–12393.

Romeo RD, Mueller A, Sisti HM, Ogawa S, McEwen BS, Brake WG 2003 Anxiety and fear behaviors in adult male and female C57BL/6 mice are modulated by maternal separations. Horm Behav. 43, 561–567. [PubMed: 12799173]

Roth BL, Hamblin MW, Ciaranello RD 1991 Developmental regulation of 5-HT2 and 5-HT1c mRNA and receptor levels. Brain Res Dev Brain Res. 58, 51–58 [PubMed: 2015654]

Ryabinin AE, Wang YM, Finn DA 1999 Different levels of Fos immunoreactivity after repeated handling and injection stress in two inbred strains of mice. Pharmacol Biochem Behav. 63, 143–151. [PubMed: 10340535]

Sabol SZ, Hu S, Hamer D. 1998 A functional polymorphism in the monoamine oxidase A gene promoter. Hum Genet. 103, 273–279. [PubMed: 9799080]

Scarpa A, Tanaka A, Chiara Haden S. 2008 Biosocial bases of reactive and proactive aggression: The roles of community violence exposure and heart rate. Journal of Community Psychology. 36, 969–988.

Scheggi S, Crociani A, De Montis MG, Tagliamonte A, Gambarana C. 2009 Dopamine D1 receptor-dependent modifications in the dopamine and camp-regulated phosphoprotein of Mr 32 kDa phosphorylation pattern in striatal areas of morphine-sensitized rats. Neuroscience 163(2), 627–639 [PubMed: 19559764]

Semple BD, Blomgren K, Gimlin K, Ferriero DM, Noble-Haeusslein LJ 2013 Brain development in rodents and humans: Identifying benchmarks of maturation and vulnerability to injury across species. Prog Neurobiol. 106–107, 1–16.

Shader M "Risk factors for delinquency: An overview", (U.S. Department of Justice, Office of Juvenile Justice and Delinquency Prevention; 2003 http://www.ncjrs.gov/html/ojjdp/jjjournal_2003_2/index.html)

Shepherd J, Farrington D, Potts J. 2004 Impact of antisocial lifestyle on health. J Public Health 26, 347–352.

Sher L, Siever LJ, Goodman M, McNamara M, Hazlett EA, Koenigsberg HW, New AS 2015 Gender differences in the clinical characteristics and psychiatric comorbidity in patients with antisocial personality disorder. Psychiatry Res. 229, 685–689. [PubMed: 26296756]

Shih JC, Ridd MJ, Chen K, Meehan WP, Kung MP, Seif I, De Maeyer E. 1999 Ketanserin and tetrabenazine abolish aggression in mice lacking monoamine oxidase A. Brain Res. 835, 104–112. [PubMed: 10415365]

Sood A, Pati S, Bhattacharya A, Chaudhari K, Vaidya VA 2018 Early emergence of altered 5-HT(2A) receptor-evoked behavior, neural activation and gene expression following maternal separation. Int J Dev Neurosci. 65, 21–28. [PubMed: 29037912]

Stone MH 2007 Violent crimes and their relationship to personality disorders. Personality and Mental Health 1, 138–153.

von Borries AKL, Volman I, de Bruijn ER, Bulten BH, Verkes RJ, Roelofs K. 2012 Psychopaths lack the automatic avoidance of social threat: relation to instrumental aggression. Psychiatry Res. 200, 761–766. [PubMed: 22819277]

Whitehead CME, Stockdale JE, Razzu G "The Economic and Social Costs of Antisocial Behaviour: A Review". London School of Economics, 2003.

Wilber AA, Southwood CJ, Wellman CL 2009 Brief neonatal maternal separation alters extinction of conditioned fear and corticolimbic glucocorticoid and NMDA receptor expression in adult rats. Dev Neurobiol. 69,73–87. [PubMed: 19025931]

Yadav PN, Kroeze WK, Farrell MS, Roth BL 2011 Antagonist functional selectivity: 5-HT2A serotonin receptor antagonists differentially regulate 5-HT2A receptor protein level in vivo. J Pharmacol Exp Ther. 339, 99–105. [PubMed: 21737536]

Yu Q, Teixeira CM, Mahadevia D, Huang Y, Balsam D, Mann JJ, Gingrich JA, Ansorge MS 2014 Dopamine and serotonin signaling during two sensitive developmental periods differentially impact adult aggressive and affective behaviors in mice. Mol Psychiatry 19, 688–698. [PubMed: 24589889]

Highlights

- Antisocial behavior (ASB) is predisposed by gene x environment interactions (GEIs)

- The best-known GEI occurs between low-activity *MAOA* alleles and child maltreatment

- We developed the first mouse model of this GEI and studied its underlying mechanism

- MAOA-hypomorphic mice subjected to early-life stress develop ASB-related phenotypes

- Our data suggest that this GEI is mediated by 5-HT2A receptors
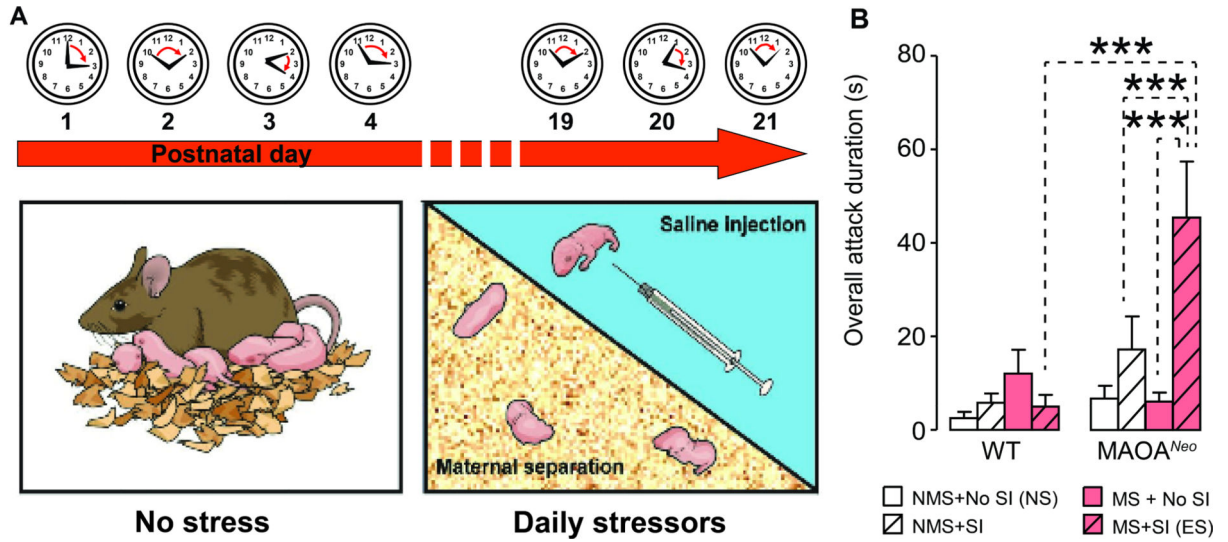
Figure 1. Validation of Gene × Environment model of ASB.
(A) Schematic diagram of the early-stress paradigm. Pups were subjected to maternal separation, daily intraperitoneal injections of saline solution, or their combination. Stressors were administered at different times and for various durations during the first three postnatal weeks, following a pseudorandom order to ensure unpredictability. **(B)** Effects of different early-life stressors on aggressive behaviors in adult MAOA^{Neo} and wildtype (WT) mice. MAOA^{Neo} pups exposed to an early stress (ES) regimen, consisting of the combination of early maternal separation (MS) and daily saline intraperitoneal injections (SI), developed a significant increase in aggression, as verified by their response towards foreign intruders in adulthood (postnatal day 80). A significant genotype × stress interaction was shown to reflect significant differences between MAOA^{Neo} mice exposed to ES and MAOA^{Neo} mice subjected to either MS or SI alone, or WT animals subjected to ES. NS, no stress. Data are shown as means ± SEM. ***, $P<0.001$ for all comparisons indicated by dotted lines (interactions). $n=11–12$/group.
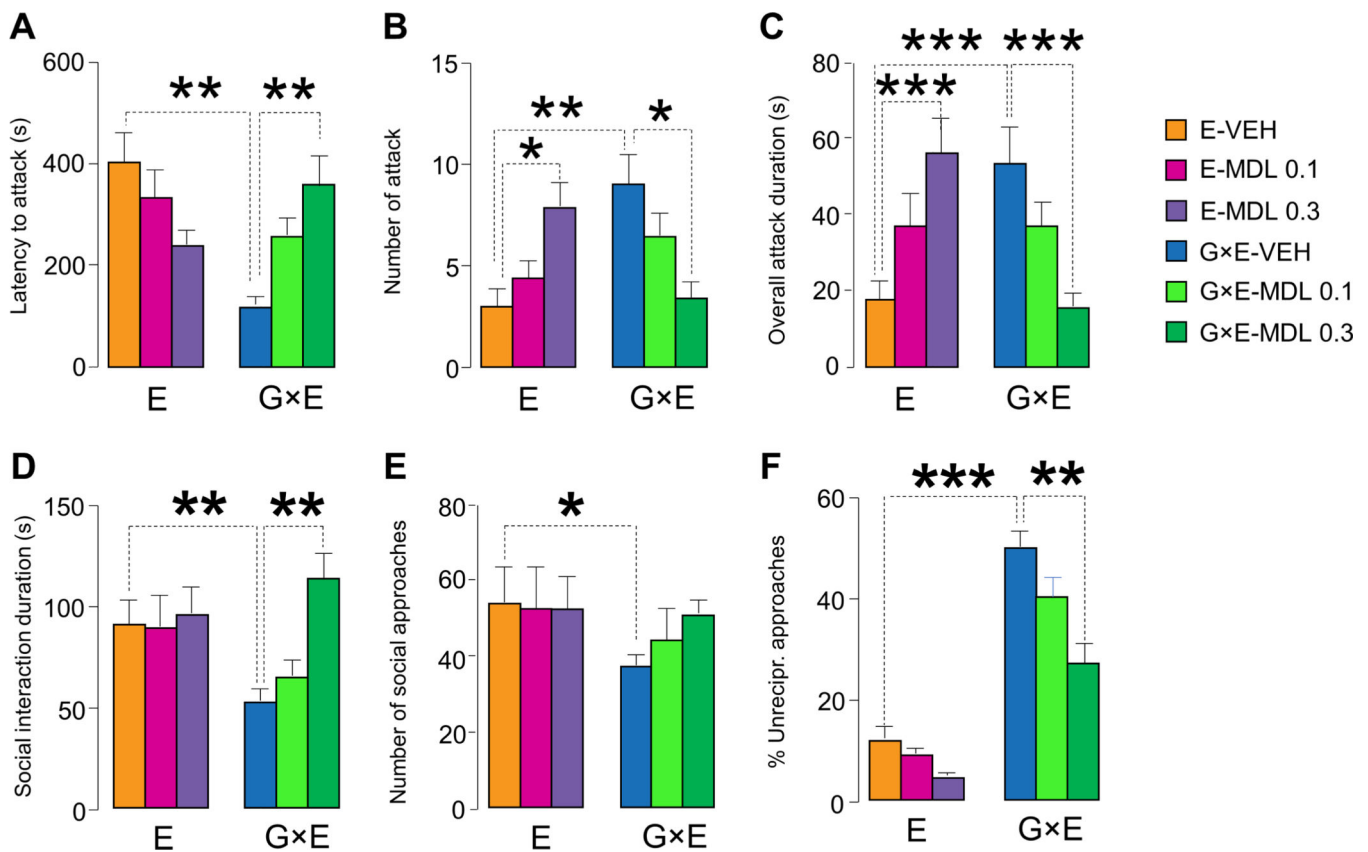
Figure 2. Definition of the critical time window for gene × environment interactions.

When tested in the resident-intruder paradigm, MAOA^{Neo} mice exposed to early stress during the first week (postnatal days 1–7, PND 1–7) exhibited (**A**) a reduced latency to attack in comparison with their wild type (WT) and unstressed controls (*Ps*<0.05); conversely, the same regimen during the second week did not elicit any overt reduction in aggression latency in MAOA^{Neo} mice. In line with these results, stress during the first week led to increased (**B**) numbers of fighting episodes and (**C**) overall fighting duration in MAOA^{Neo} mice, as compared to both unstressed mice and mice stressed during the second week. The analysis of social interactions in a novel cage also showed that early stress exposure did not modify the number of social approaches (**D**) or their overall duration (**E**), irrespective of the week of administration; however, main effects for genotype indicated that MAOA^{Neo} mice exhibited a reduction in both parameters. Finally, (**F**) MAOA^{Neo} mice subjected to stress during the first, but not second postnatal week, exhibited a significant increase in non-reciprocal responses towards the approaches initiated by the conspecifics. Data are shown as means ± SEM. *, *P*<0.05; **, *P*<0.01; ***, *P*<0.001 for all comparisons indicated by dotted lines (interactions). #, *P*<0.05 for all comparisons between brackets indicated by dotted lines (Main effect). *n*=13–15/group.
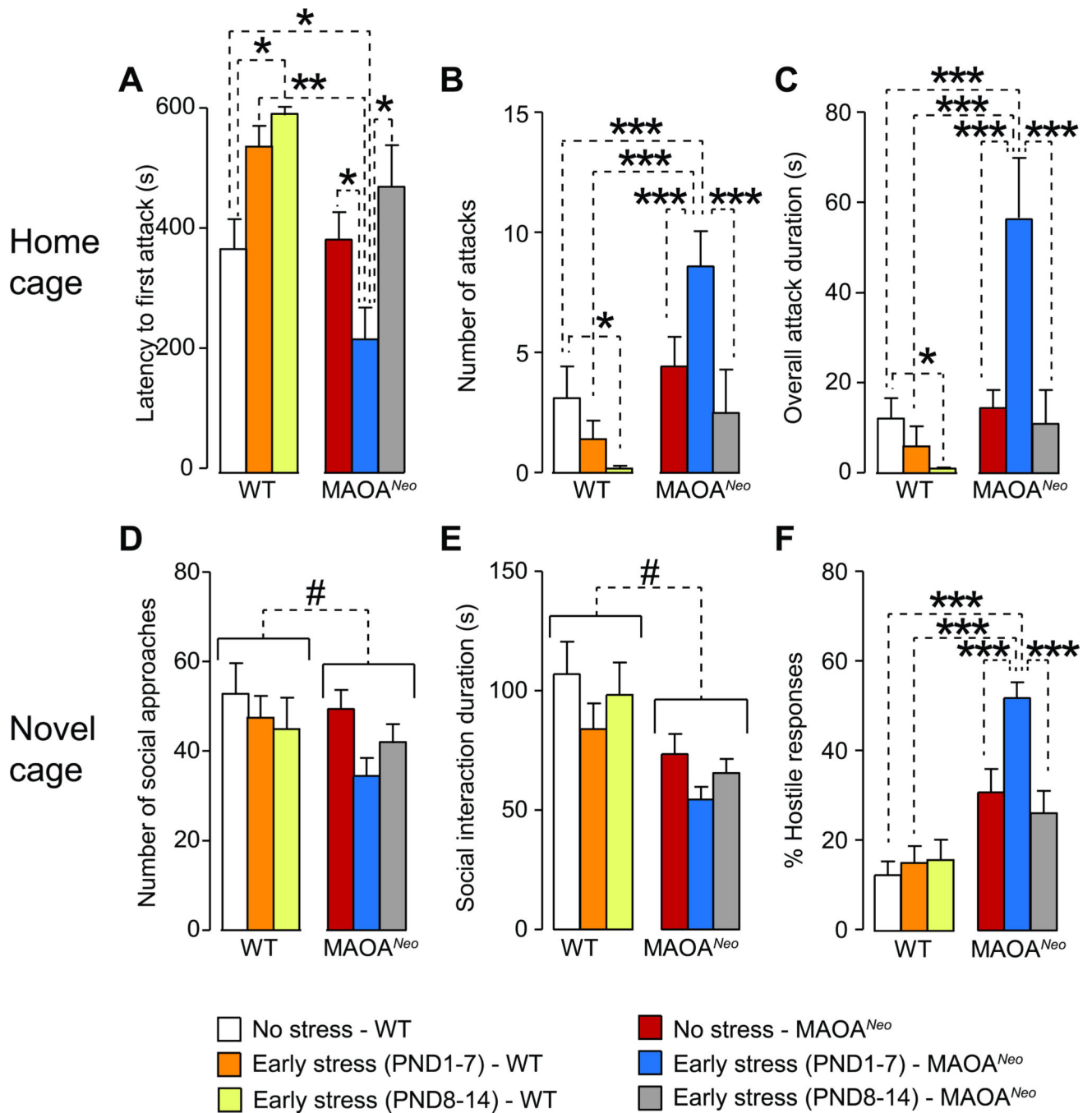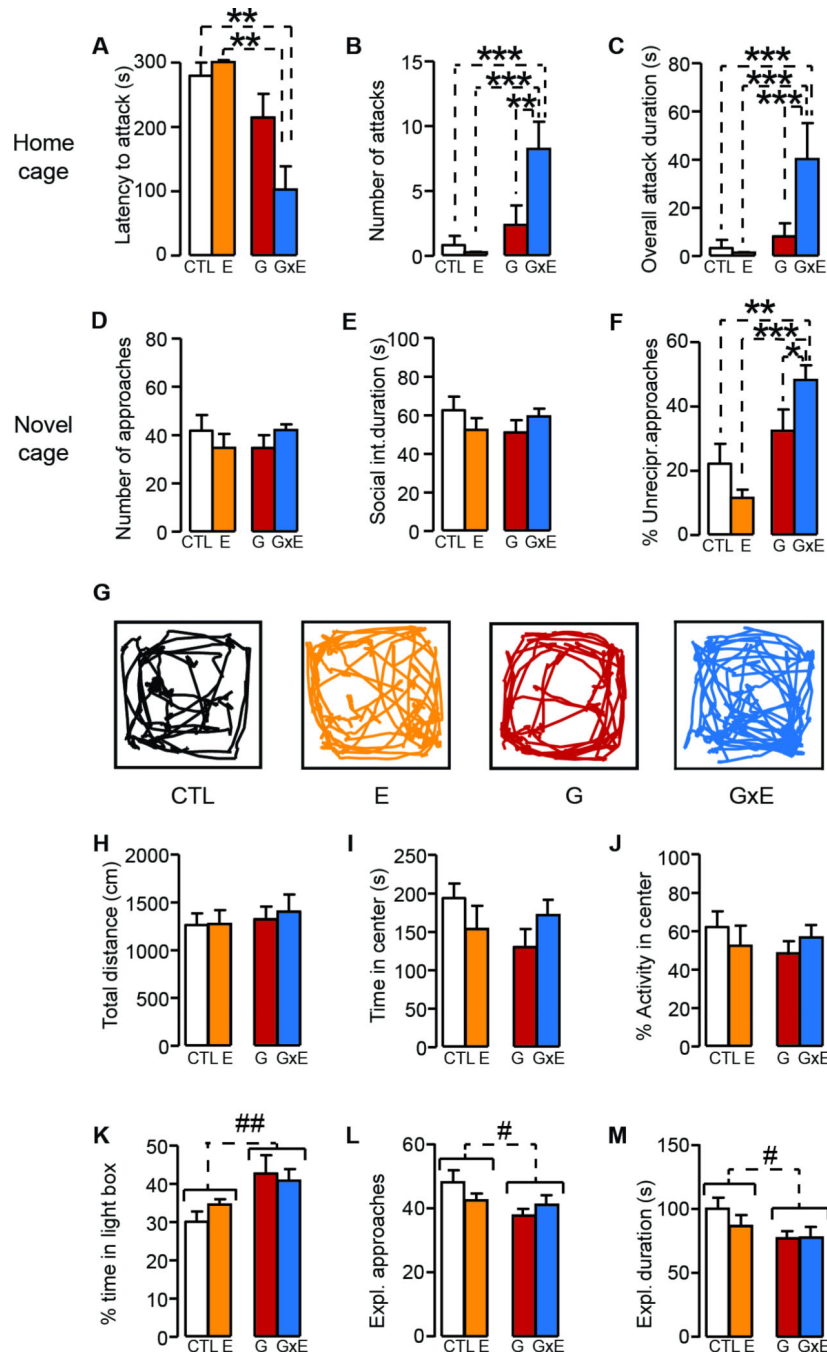
Figure 3. Behavioral phenotype of GxE mice at PND 80.

The analysis of locomotor activity (**A** shows representative locomotor tracings) in the open-field test revealed (**B**) a significant genotype-specific reduction in total distance (n= 10/group); however, no interactions between genotype and environment were found; additionally, no differences were detected with respect to (**C**) the time spent or (**D**) % locomotor activity in the center of the arena. No difference among groups was detected for (**E**) startle amplitude and for (**F**) prepulse inhibition (PPI) (n= 9–10/group). While all MAOA^{Neo} mice displayed (**G**) a significant decrease in spontaneous alternations in the T

maze, irrespective of their early stress exposure (n=9/group), no interactions between genotype and environment were found. (**H**) In the light-dark box paradigm, no genotype × environment interactions were detected with respect to the time spent in the lit compartment (n= 8/group). (**I**) In the novel object exploration task, MAOA^{Neo} males exhibited a genotype-specific reduction in object exploratory duration, irrespective of their early stress exposure (n= 11–12/group). In contrast, (**J**) the analysis of immobility in the tail suspension test revealed a significant genotype × stress interaction (n=18–19/group); post-hoc analyses revealed that this effect depended on a significant increase in immobility in stressed wild-type (*E*) mice, as compared to non-stressed controls (*CTL;* P<0.05*)*, as well as a reduction in immobility in mice subjected to early stress *(G×E),* as compared with their unstressed MAOA^{Neo} counterparts (*G*). Finally, in the predator-cued emergence test (**K**), *G×E* animals showed an increased propensity to enter the areas outside their enclosure and approach the anesthetized rat (**L**), as signified by (**M**) their reduced latency to enter the area occupied by the rat, as well as a longer time spent in (**N**) the rat area and (**O**) on the body of the rat itself (n=9/group). Data are shown as means ± SEM. *, *P*<0.05; **, *P*<0.01; ***, *P*<0.001 for all comparisons indicated by dotted lines (interactions). #, *P*<0.05 for all comparisons between brackets indicated by dotted lines (Main effect).
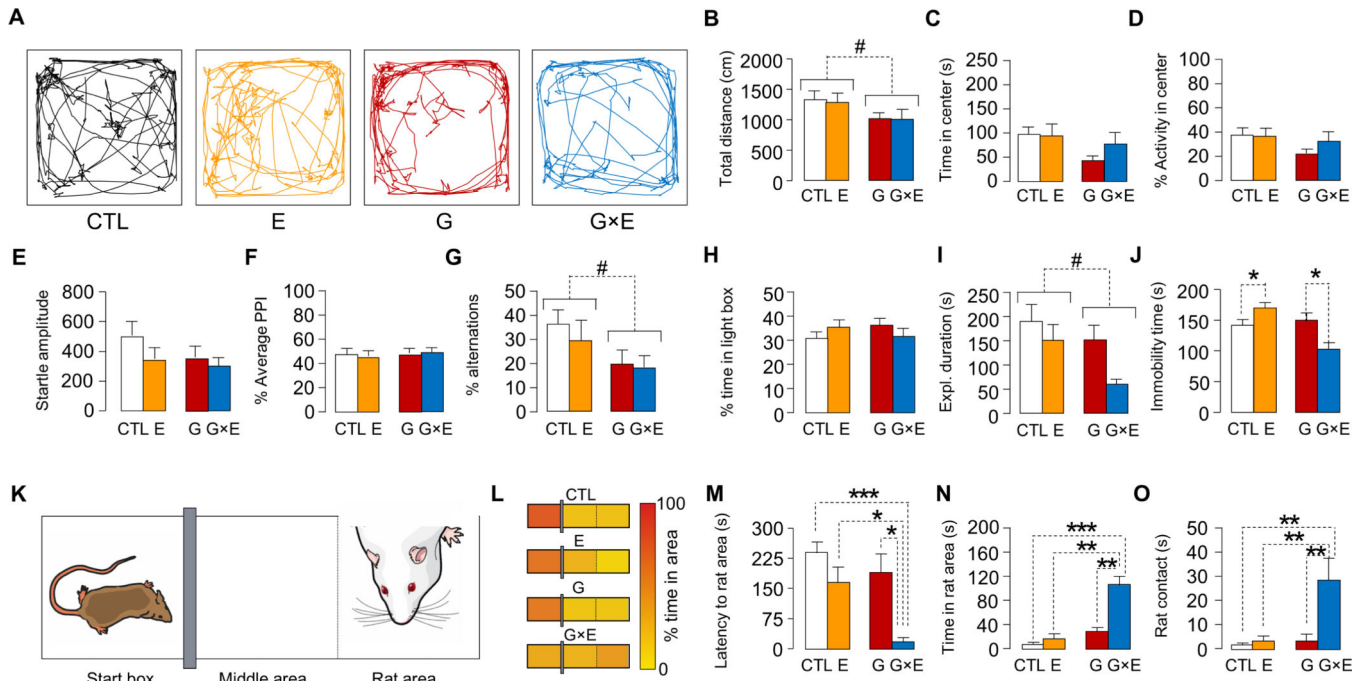
Figure 4. Behavioral phenotype of G × E mice at postnatal day 28.

The analysis of home-cage intermale aggression in 28-day old mice (**A-C**) revealed that MAOA^Neo^ mice subjected to early stress exhibited significant increases in fighting behaviors. In the social interaction test, no differences were found with respect to (**D**) the number and (**E**) duration of social approaches. (n = 10/group). Conversely, these mice also exhibited (**F**) a significant increase in non-reciprocal responses. The analysis of locomotor activity in the open field (**G**) did not identify any changes in (**H-J**) locomotor activity (n= 9/group). (**K**) In the light-dark box, MAOA^Neo^ mice spent more time in the lit compartment, irrespective of early stress exposure (n= 9–10/group); however, no specific interaction was found between genotype and early-stress exposure. Furthermore, no differences in chamber transitions were found among groups. Novel-object-exploration analyses indicated a reduction in the number of approaches (**L**) and overall duration (**M**) of this behavior in MAOA^Neo^ mice, irrespective of early stress exposure (n= 9–10/group); however, no interactions were detected between genotype and stress. Data are shown as means ± SEM. *, $P<0.05$; **, $P<0.01$; ***, $P<0.001$ for all comparisons indicated by dotted lines (interactions). #, $P<0.05$; ##, $P<0.01$ for all comparisons between brackets indicated by dotted lines (Main effect). Abbreviations: CTL, unstressed wild type (WT) mice; E, WT mice subjected to early stress during the first postnatal week; *G*, unstressed MAOA^Neo^ mice; *G×E*, MAOA^Neo^ mice subjected to early stress during the first postnatal week.

Figure 5. Gene × environment effects on neuromorphological and developmental features in mouse pups at postnatal day 7.

The analysis of (**A**) the developmental trajectory of body weight in mouse pups revealed no significant G×E interactions (n= 6–7/group); however, MAOA^{Neo} mice displayed a slight, yet significant reduction in this parameter, irrespective of early stress exposure (**B-C**). The analysis of neurological reflexes during the first postnatal week (n=6/group) showed a significant difference in the righting, but not geotaxis reflex (Mantel-Cox log-rank). In particular, unstressed wild type mice (*CTL*) displayed a significantly faster acquisition of the

righting reflex than stress-exposed wild-type (*E)*, unstressed MAOA*Neo (G)* and stressed MAOA*Neo* pups *(G×E). G×E* pups also showed a delayed righting reflex compared to *E* littermates. In addition to these studies, morphological analyses of the brains on PND 8 (**D**: representative picture of sampled areas in the prefrontal cortex; **E**: Digital micrographs of cresyl echt violet-stained coronal sections of mouse pups; **F**: digital micrographs of cresyl echt violet-stained horizontal sections of the orbital frontal cortex) failed to reveal any overt differences between groups. Specifically, comparisons of (**G**) thickness across different cortical layers harboring pyramidal neurons and (**H**) soma volume of these cells did not show any differences between groups (3-way ANOVA; n=6–7/group). Data are shown as means ± SEM. #, *P*<0.05 for all comparisons between brackets indicated by dotted lines (Main effect).
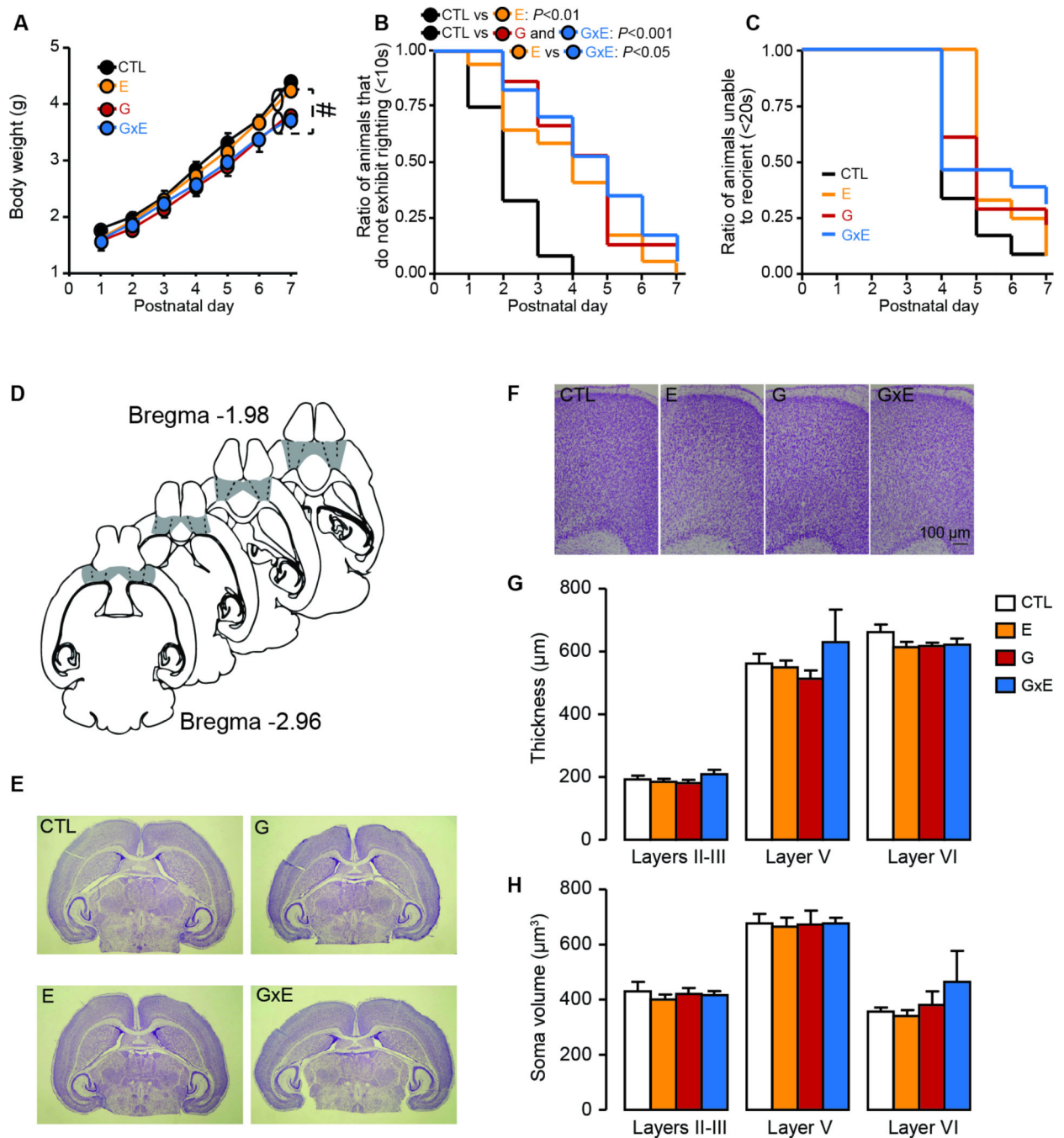
Figure 6. Early predictors of antisocial-related behaviors in G × E mice.

(**A-D**) Actometric analyses on pups at PND 8 [(**A**) shows representative pathways for each group)] revealed that both stressed and unstressed MAOA^{Neo} pups displayed greater locomotor activity, as shown by (**B**) the higher total distance (n=9–10/group), (**C**) the reduced number of low-mobility bouts, and (**D**) the higher vertical force (2-way ANOVA). However, no genotype × environment interactions were found (n=9–10/group). (**E**) Analyses of ultrasonic vocalizations also revealed a significant reduction in MAOA^{Neo} pups, irrespective of their stress exposure (n=15/group); however, no G×E interactions were found.

Conversely, ECG analyses [(**F**) shows representative tracks for each group] indicated that *G×E* pups displayed a significant reduction in resting heart rate, as measured by (**G**) an increase in the inter-beat interval (n=14–15); this effect was not due to dysfunctions in heart dynamics, as indicated by (**H**) equivalent values in QRS/RR ratios (2-way ANOVA). Data are shown as means ± SEM. &, *P*<0.05 vs WT mice exposed to no stress (*CTL*); *, *P*<0.05; **, *P*<0.01; ***, *P*<0.001 for all comparisons indicated by dotted lines (interactions). ##, *P*<0.01; ###, *P*<0.001 for all comparisons between brackets indicated by dotted lines (Main effect). Abbreviations: CTL, unstressed wild type (WT) mice; E, WT mice subjected to early stress during the first postnatal week; *G,* unstressed MAOA^{Neo} mice; *G×E*, MAOA^{Neo} mice subjected to early stress during the first postnatal week.
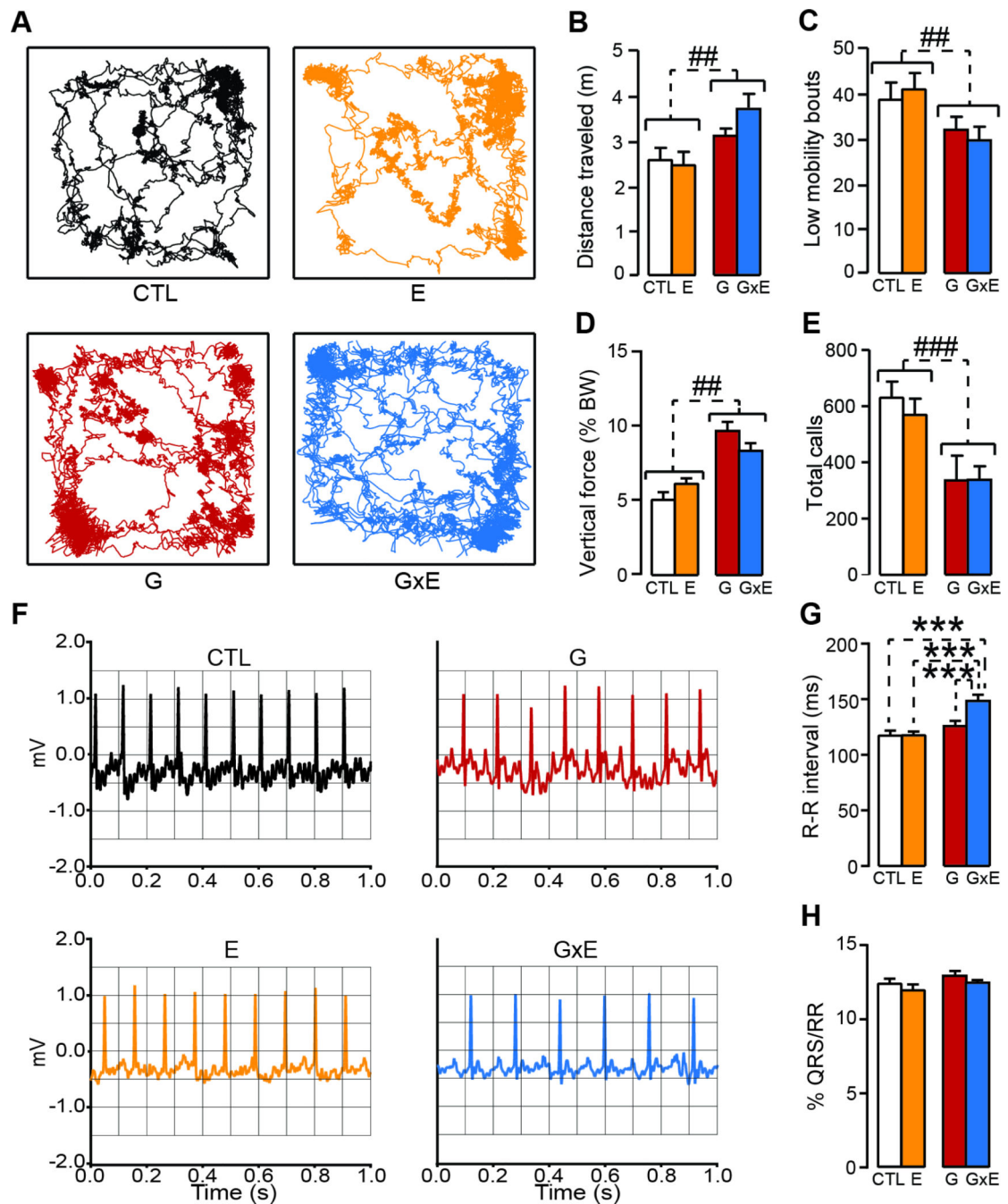
Figure 7. Low-activity *Maoa* genotype and early stress on monoamine levels and serotonin receptor subtypes in the prefrontal cortex (PFC) of pups at postnatal day 7.
The analysis of monoamine levels in the PFC in mouse pups (PND 8) revealed that MAOA^{Neo} pups displayed (**A**) a dramatic elevation in forebrain serotonin (5-HT) levels, irrespective of their stress exposure (2-way ANOVA; n=8/group); however, no G×E differences were detected. Similar, albeit much milder effects were found for (**B**) norepinephrine (NE) levels (2-way ANOVA); no significant genotype × environment interactions were found for either 5-HT or NE. Finally, (**C**) no significant differences were found for dopamine levels (2-way ANOVA, n=7/group). Western blot analyses of serotonin

receptor levels in the PFC on PND 8 revealed no differences for **(D)** 5-HT$_{1A}$ (2-way ANOVA; n=5/group), **(E)** 5-HT$_{1B}$ (2-way ANOVA; n=5/group), and **(F)** 5-HT$_{2C}$ (2-way ANOVA; n=5/group). Conversely, 5-HT$_{2A}$ levels were significantly enhanced in MAOA^{Neo} mice subjected to early stress during the first postnatal week ($G{\times}E$) (2-way ANOVA; n=6/ group). Data are shown as means ± SEM. *, $P{<}0.05$ for all comparisons indicated by dotted lines (interactions). $^{\#\#\#}$, $P{<}0.001$ for all comparisons between brackets indicated by dotted lines (Main effect). Abbreviations: CTL, unstressed wild type (WT) mice; E, WT mice subjected to early stress during the first postnatal week; G, unstressed MAOA^{Neo} mice; $G{\times}E$, MAOA^{Neo} mice subjected to early stress during the first postnatal week.
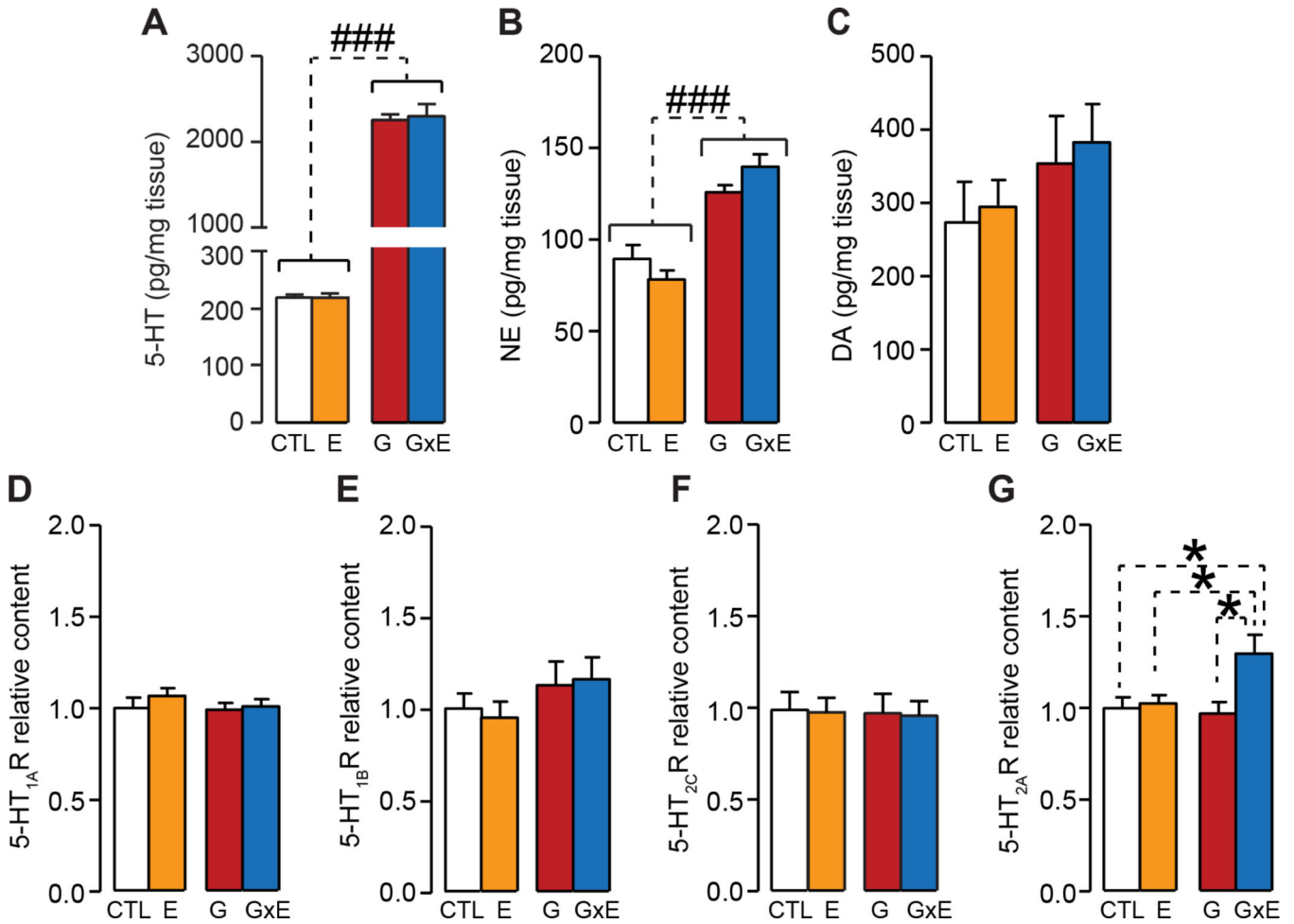
Figure 8. G×E pups show elevated 5-HT$_{2A}$ receptor staining in the orbitofrontal cortex at postnatal day 7.

(**A-B**) Digital light micrographs and percent intensity of staining of 5-HT$_{2A}$ receptor immunopositive cells in the orbitofrontal cortex (**C-D**) Digital light micrographs and percent intensity of staining of 5-HT$_{2A}$ receptor immunopositive cells in the temporal-occipital cortex at postnatal day 8. Immunohistochemical studies revealed that (**A-B**) 5-HT$_{2A}$ levels were significantly enhanced in the orbitofrontal cortex of stress-subjected MAOA^{Neo} pups (3-way ANOVA; n=7/group); conversely (**C-D**), no differences were found in the temporal-occipital cortex (3-way ANOVA; n= 7/group). Data are shown as means ± SEM. Scale bar is set at 25 μm. *, $P<0.05$ for all comparisons indicated by dotted lines (interactions). Abbreviations: CTL, unstressed wild type (WT) mice; E, WT mice subjected to early stress during the first postnatal week; *G,* unstressed MAOA^{Neo} mice; *G×E*, MAOA^{Neo} mice subjected to early stress during the first postnatal week.
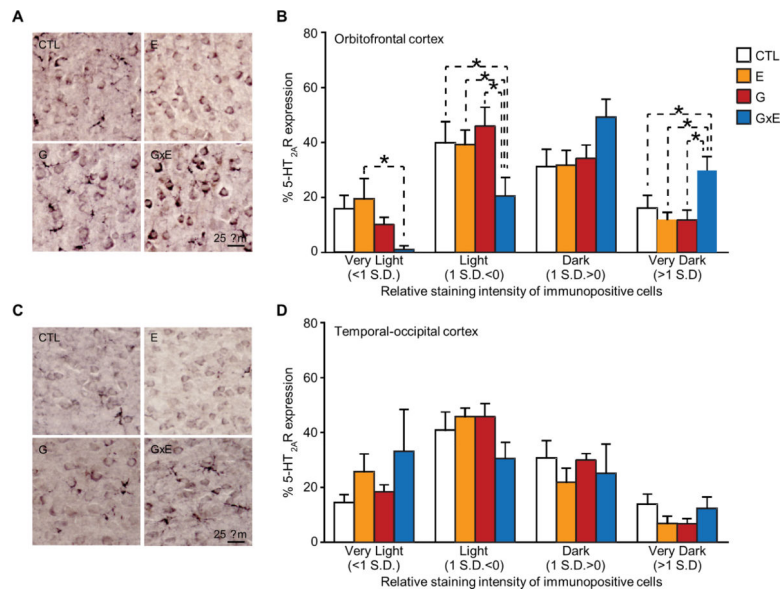
Figure 9. Treatment with the 5-HT$_2$ receptor antagonist ketanserin (KET, 1 and 3 mg kg^{-1}, IP) during the first postnatal week prevents aggressive behavior of G×E mice.

(**A-C**) KET rescued resident-intruder aggression (n=10/group) in MAOA^{Neo} mice subjected to early stress (*G×E*), but not in stressed WT littermates (*E*). In a novel cage (n=8/group), *G×E* mice treated with KET engaged in (**D**) longer duration and (**E**) greater number of social approaches and exhibited (**F**) fewer asocial behaviors in response to social approaches initiated by the social counterpart (2-way ANOVA). Data are shown as means ± SEM. *, *P*<0.05; **, *P*<0.01; ***, *P*<0.001 for all comparisons indicated by dotted lines (interactions). *n*=11–12/group.
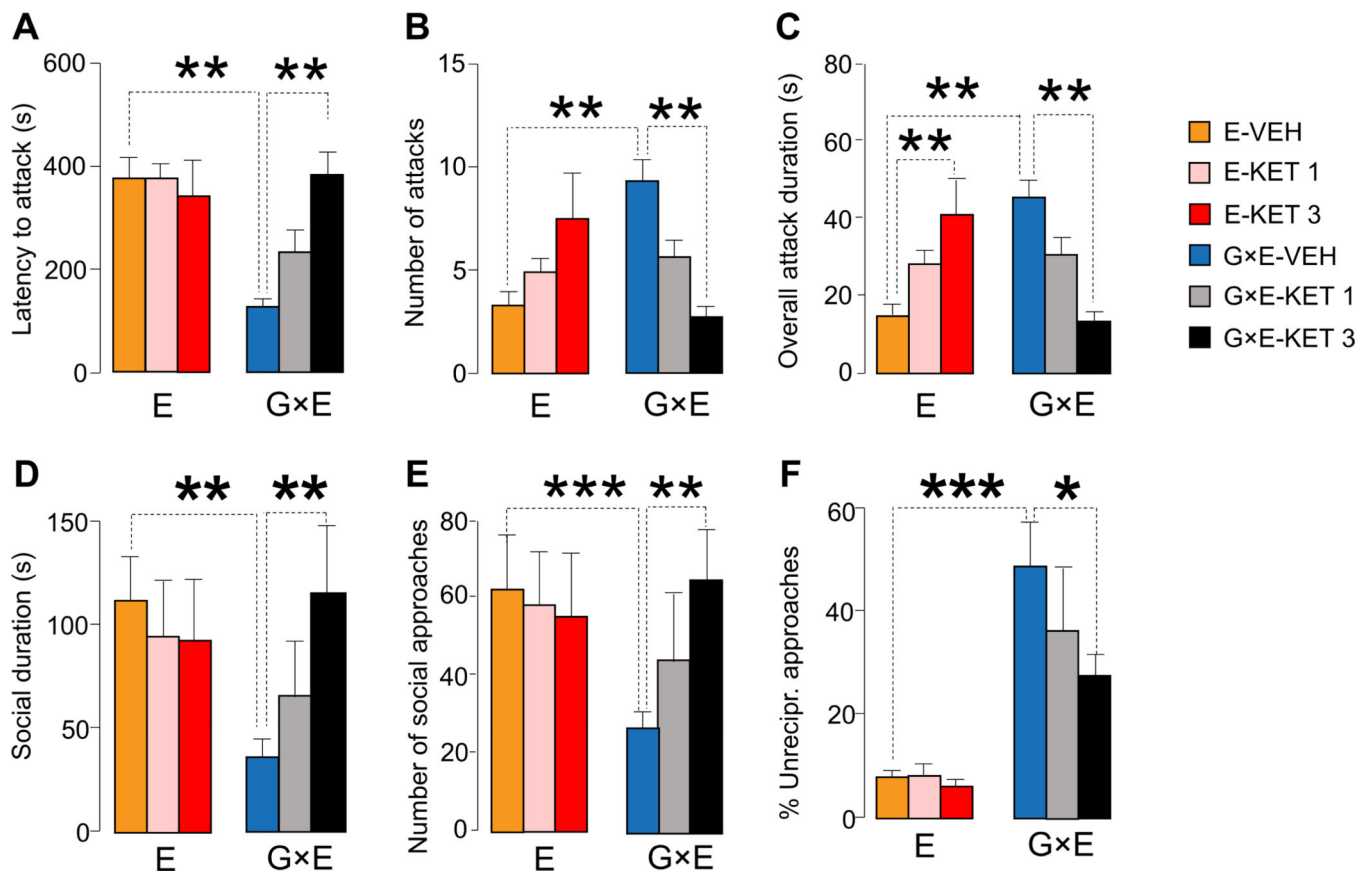
Figure 10. Treatment with the selective 5-HT$_{2A}$ receptor antagonist MDL-100,907 (MDL, 0.1 and 0.3 mg kg^{-1}, IP) during the first postnatal week prevents aggressive behavior of G×E mice.
(**A-C**) MDL rescued resident-intruder aggression in MAOA^{Neo} mice subjected to early stress (*G×E*), and surprisingly produced opposite results in stressed wild type littermates (*E*). In a novel cage (n=8/group), *G×E* mice treated with MDL engaged in (**D**) longer duration, but not overall number of (**E**) social approaches and exhibited (**F**) a lower proclivity to reciprocate social approaches initiated by their social counterparts (2-way ANOVA). Data are shown as means ± SEM. *, *P*<0.05; **, *P*<0.01; ***, *P*<0.001 for all comparisons indicated by dotted lines (interactions).